

**REDUCTION OF TOTAL SUSPENDED SOLIDS, TURBIDITY AND
COLOUR FROM PALM OIL MILL EFFLUENT USING HYBRID
COAGULATION-ULTRAFILTRATION PROCESS**

NG WEI QUAN

**A project report submitted in partial fulfilment of the
requirements for the award of Bachelor of Engineering
(Hons.) Chemical Engineering**

**Lee Kong Chian Faculty of Engineering and Science
Universiti Tunku Abdul Rahman**

August 2018

DECLARATION

I hereby declare that this project report is based on my original work except for citations and quotations which have been duly acknowledged. I also declare that it has not been previously and concurrently submitted for any other degree or award at UTAR or other institutions.

Signature : _____

Name : Ng Wei Quan

ID No. : 14UEB00251

Date : 14/9/2018

APPROVAL FOR SUBMISSION

I certify that this project report entitled “**REDUCTION OF TOTAL SUSPENDED SOLIDS, TURBIDITY AND COLOUR FROM PALM OIL MILL EFFLUENT USING HYBRID COAGULATION-ULTRAFILTRATION PROCESS**” was prepared by **NG WEI QUAN** has met the required standard for submission in partial fulfilment of the requirements for the award of Bachelor of Engineering (Hons.) Chemical Engineering at Universiti Tunku Abdul Rahman.

Approved by,

Signature : _____

Supervisor : Dr. Lai Soon Onn

Date : 14/9/2018

The copyright of this report belongs to the author under the terms of the copyright Act 1987 as qualified by Intellectual Property Policy of Universiti Tunku Abdul Rahman. Due acknowledgement shall always be made of the use of any material contained in, or derived from, this report.

© 2018, Ng Wei Quan. All right reserved.

ACKNOWLEDGEMENTS

I would like to thank everyone who had contributed to the successful completion of this project. I would like to express my gratitude to my research supervisor, Dr. Lai Soon Onn for his invaluable advice, guidance and his enormous patience throughout the development of the research.

In addition, I would also like to express my gratitude to my loving parents and friends who had helped and given me encouragement in completing this final year project. A token of appreciation is also forwarded to both laboratory officers, Mr Jung Seow Yung and Ms Amalina Nabilah binti Ahmad Bakhi. They have always been very helpful in giving me guidance in usage of laboratory equipment.

I would also like to credit Mr Lim Su Wei, a postgraduate student in UTAR for his guidance and invaluable knowledge pertaining to membranes which had helped me throughout this research project.

ABSTRACT

High consumption and production of palm oil have led to the massive generation of palm oil mill effluent (POME). The discharge of POME has brought impacts to environment and human health by polluting surface water. This study was intended to reduce the total suspended solids (TSS), turbidity and colour using hybrid coagulation-ultrafiltration process. POME was pre-treated with coagulation process using polyaluminium chloride (PAC) and the optimization of operating condition for coagulation process was performed. The coagulation results revealed that the optimum pH, dosage of coagulant and rapid mixing speed were pH 4, 600mg/L and 200 rpm, respectively. It achieved the highest percent reduction of TSS, turbidity and colour with 99.74%, 94.44% and 94.6%, respectively. Ultrafiltration (UF) membrane was fabricated using polyestersulfone (PES) as a base polymer, polyvinylpyrrolidone (PVP) as additive and titanium dioxide (TiO₂) nanoparticle. Different concentrations ranging from 0.00, 0.1, 0.5, and 1.0 wt% of TiO₂ nanoparticles were added into the dope solution. The cross-sectional structure, pure water permeability, pore size and porosity of the UF membranes were examined. The characterization studies confirmed that higher concentration of TiO₂ provided higher pure water permeability and more porous structure in the UF membranes. The effect of concentration of TiO₂ and transmembrane pressure (TMP) on permeate flux and reduction of TSS, turbidity and colour were studied. The amount of TiO₂ in membrane only affected the permeate flux but had no obvious effects on the reduction of TSS, turbidity and colour. The optimum TMP was found to be 3 bar, resulting in the greatest reduction of TSS, turbidity and colour. The overall percent reduction for TSS, turbidity and colour using hybrid-coagulation process were found to be 99.95%, 99.21% and 98.60%, respectively. Total suspended solids were found to have strong relationship between turbidity and colour. However, turbidity and colour in POME might be contributed by other factors as they do not achieve a high reduction efficiencies when total suspended solids were removed.

TABLE OF CONTENTS

DECLARATION	ii
APPROVAL FOR SUBMISSION	iii
ACKNOWLEDGEMENTS	v
ABSTRACT	vi
TABLE OF CONTENTS	vii
LIST OF TABLES	xi
LIST OF FIGURES	xii
LIST OF SYMBOLS / ABBREVIATIONS	xiv
LIST OF APPENDICES	xvi

CHAPTER

1	INTRODUCTION	1
	1.1 Background	1
	1.2 Problem Statement	2
	1.3 Aim and Objectives	3
	1.4 Scope and Limitation of the Study	3
2	LITERATURE REVIEW	5
	2.1 Characteristics of Oily Palm Oil Mill Effluent	5
	2.2 Coagulation as Pre-treatment	6
	2.2.1 Colloidal Particles	7
	2.3 Classifications of Coagulants	7
	2.3.1 Chemical Coagulants	7
	2.3.2 Natural Coagulants	8
	2.4 Conditions Affecting Performance of Coagulation	8
	2.4.1 pH of Solutions	8
	2.4.2 Dosage of Coagulants	9

2.4.3	Rapid Mixing Speed	9
2.5	Basics of Membrane Technology	9
2.5.1	Microfiltration	12
2.5.2	Ultrafiltration	13
2.5.3	Nanofiltration	13
2.5.4	Reverse Osmosis	13
2.5.5	Hybrid Membrane Process	14
2.6	Membrane Materials	14
2.7	Hydrophilicity of Membrane	15
2.8	Parameters Affecting the Performance of Membrane Process	16
2.8.1	Transmembrane Pressure	16
2.8.2	pH of Feed Solution	17
2.8.3	Oil Concentration	17
2.8.4	Temperature of Feed Solution	17
2.9	Membrane Fouling	18
2.10	Cleaning of Fouled Membrane	18
3	METHODOLOGY AND WORK PLAN	20
3.1	Methodology Introduction	20
3.1.1	Materials	20
3.2	Coagulation using Polyaluminium Chloride (PAC)	21
3.2.1	Optimum Coagulant Dosage	21
3.2.2	Optimum pH	22
3.2.3	Optimum Rapid Mixing Speed	22
3.3	Membrane Fabrication	22
3.3.1	Dope Solution Preparation	22
3.3.2	Membrane Casting	23
3.4	Characterizations of Membranes	24
3.4.1	Membrane Porosity	24
3.4.2	Pore Size Distribution	24
3.4.3	Scanning Electron Microscopy (SEM) Analysis and Energy-dispersive X- ray Spectroscopy (EDX) Analysis	25

3.4.4	Fourier Transform Infrared Spectroscopy (FTIR)	26
3.4.5	Pure Water Permeability	26
3.5	Membrane Filtration	27
3.5.1	Experimental Setup	27
3.5.2	Transmembrane Pressure	27
3.5.3	Permeate Flux	28
3.6	Determination of Total Suspended Solids	28
3.7	Determination of Colour	29
3.8	Determination of Turbidity	30
4	RESULTS AND DISCUSSION	31
4.1	Optimization of Operating Conditions for Coagulation Process	31
4.1.1	Optimum pH condition	31
4.1.2	Optimum PAC Dosage	32
4.1.3	Optimum Rapid Mixing Speed	33
4.2	Characterization of Fabricated Membranes	33
4.2.1	Cross-Sectional Morphology	33
4.2.2	Fourier Transform Infrared Spectroscopy (FTIR) Results	35
4.2.3	Energy Dispersive X-ray Spectroscopy (EDX)	37
4.2.4	Porosity and Pore Size Distribution Results	37
4.2.5	Pure Water Permeability Results	38
4.3	Membrane Filtration Results	39
4.3.1	Effect of TiO ₂ Loading on Permeate Flux	39
4.3.2	Effect of TiO ₂ Loading on Reduction of Total Suspended Solids, Turbidity and Colour	40
4.3.3	Effect of Transmembrane Pressure on Permeate Flux	41
4.3.4	Effect of Transmembrane Pressure on Reduction of Total Suspended Solids, Turbidity and Colour	42
4.4	Overall Reduction Percentage for Hybrid Process	45

4.5	Correlation of Total Suspended Solids, Turbidity and Colour	46
5	CONCLUSIONS AND RECOMMENDATIONS	48
5.1	Conclusions	48
5.2	Recommendations for Future Work	49
	REFERENCES	50
	APPENDICES	56

LIST OF TABLES

Table 2.1: Characteristics of Palm Oil Mill Effluent	5
Table 2.2: Effluent Standards for Palm Oil Mill	6
Table 2.3: Examples of Membrane Processes with Different Driving Force	10
Table 2.4: Advantages and Disadvantages for Membrane with Different Driving Forces	12
Table 2.5: Common Types of Chemical Cleaning Agents with Advantages and Disadvantages	19
Table 3.1: Materials required for the experiment with their respective function	20
Table 3.2: Compositions of Dope Solution for Ultrafiltration Membranes	22
Table 4.1: Weight Percent (wt%) of Membranes	37
Table 4.2: Atomic Percent (At%) of Membranes	37
Table 4.3: Porosity and Pore Size of Membranes	38

LIST OF FIGURES

Figure 2.1: Characteristics of Different Pressure Driven Membranes	11
Figure 2.2: Contact Angle for Hydrophilic and Hydrophobic Membranes	15
Figure 3.1: Flocculation Test Unit (LS-260001-A)	21
Figure 3.2: Ultrasonic Cleaner (SK5200GT, KUDOS)	23
Figure 3.3: Scanning Electron Microscopy (S-3400N, Hitachi)	25
Figure 3.4: Sputter Coater (SC7620, EMITECH)	25
Figure 3.5: FTIR Instrument (IS10, NICOLET)	26
Figure 3.6: Schematic Diagram of Dead End Filtration System	27
Figure 3.7: HACH DR 3900 Spectrophotometer	29
Figure 3.8: Turbidity Meter (TN-100, Eutech Instruments)	30
Figure 4.1: Percent Reduction for Total Suspended Solids, Turbidity and Colour at different pH under 600 mg/L coagulant dosage and 150 rpm rapid mixing speed	31
Figure 4.2: Percent Reduction for Total Suspended Solids, Turbidity and Colour at Different Coagulant Dosage under pH 4 and 150 rpm Rapid Mixing Speed	32
Figure 4.3: Percent Reduction for Total Suspended Solids, Turbidity and Colour at Different Rapid Mixing Speed under pH 4 and 600 mg/L Coagulant Dosage	33
Figure 4.4: SEM Micrographs of Cross-Sectional Structure for Membranes U1, U2, U3 and U4 at Magnification of 2000x	34
Figure 4.6: FTIR Spectrum for Different Types of Membranes	36
Figure 4.7: Pure Water Permeability of Membranes under Transmembrane Pressure of 1 bar	39

Figure 4.8: Permeate Flux for Different Types of Membranes under Transmembrane Pressure of 3 bar	40
Figure 4.9: Percent Reduction of Total Suspended Solids, Turbidity and Colour for Different Types of Membranes under Transmembrane Pressure of 3 bar	41
Figure 4.10: Permeate Flux for Membrane U3 at Different Transmembrane Pressures	42
Figure 4.11: Percent Reduction of Total Suspended Solids, Turbidity and Colour for Membrane U4 under Different Transmembrane Pressures	43
Figure 4.12: Percent Reduction of Total Suspended Solids, Turbidity and Colour for Membrane U1 under Different Transmembrane Pressures	43
Figure 4.13: Percent Reduction of Total Suspended Solids, Turbidity and Colour for Membrane U2 under Different Transmembrane Pressures	44
Figure 4.14: Percent Reduction of Total Suspended Solids, Turbidity and Colour for Membrane U3 under Different Transmembrane Pressures	44
Figure 4.15: Overall Percent Reduction of Hybrid Coagulation-Ultrafiltration Process for Different Membranes under Transmembrane Pressure of 3 bar	45
Figure 4.16: Correlation between Total Suspended Solids and Turbidity	46
Figure 4.17: Correlation between Total Suspended Solids and Colour	47
Figure 4.18: Correlation between Turbidity and Colour	47

LIST OF SYMBOLS / ABBREVIATIONS

A	effective area of the membrane, m ²
C_f	concentration of feed solution, mg/L
C_p	concentration of permeate, mg/L
J	flux, L/ (m ² .h)
l	membrane thickness, m
ΔP	operational pressure, Pa
Q	volume of the permeate water per unit time, m ³ /h
R	percent reduction, %
r_m	average pore size, m
Δt	sampling time, h
w	weight of membrane, g
ε	porosity of membrane (%)
η	water viscosity at 25 °C, Pa·s
ρ	density, g/cm ³
ADMI	American Dye Manufacturer Institution
BOD	Biological Oxygen Demand
COD	Chemical Oxygen Demand
CAG	contact angle goniometer
DOE	department of environment
EDX	energy-dispersive x-ray spectroscopy
FTIR	fourier transform infrared spectroscopy
HACH	HACH Company
HCl	hydrochloric acid
MPOC	Malaysian Palm Oil Council
MWCO	molecular cut-off weight
NaOH	Sodium hydroxide
NMP	n-methyl-2-pyrrolidone
PAC	polyaluminium chloride
PES	polyethersulfone
POME	palm oil mill effluent

PTFE	polytetrafluoroethylene
PVDF	polyvinylidene fluoride
PVP	polyvinylpyrrolidone
SEM	scanning electron microscopy
TiO ₂	Titanium Dioxide
TSS	Total Suspended Solids
TMP	transmembrane pressure
UF	ultrafiltration

LIST OF APPENDICES

APPENDIX A: Coagulation Data	56
APPENDIX B: EDX Analysis	58
APPENDIX C: Wet and Dry Weight of Membranes	61
APPENDIX D: Membrane Filtration Data	62

CHAPTER 1

INTRODUCTION

1.1 Background

Development of technologies and growth of population in the world have brought up an industrial revolution. Along with the industrial revolution, amount of factories and production has increased in order to overcome the demands. However, the industrial development has produced huge amount of industrial effluents. This effluent contains high amount of solids and oil which could bring many negative effects to both human health and environment. It affects the clean water sources, harming both marine organisms and human (Yu, Han and He, 2017). Besides, it also causes atmospheric pollution and affects the crop production (Yu, Han and He, 2017).

Due to the adverse effects of industrial effluents, various method have been designed to treat different industrial effluent such as membrane separation, gas floatation, biological treatment and coagulation. Gas floatation process injects fine gas bubbles into oily wastewater to allow oil particles to attach themselves to the gas bubbles. This creates a higher density difference between the water and oil particles causing the oil particles to rise faster, resulting in a rapid and effective separation (Moosai and Dawe, 2003). Biological treatment process utilizes microbial metabolism to enable the biodegradation of organic pollutants into harmful matters which are more stable (Kriipsalu et al., 2007). For coagulation process, coagulant is added into wastewater to destabilize and aggregate colloids. It allows the formation of flocs in the wastewater which are easily settled and removed (Ahmad, Sumathi and Hameed, 2006). Membrane filtration method utilizes a thin selective barrier to achieve separation effect. Nowadays, membrane filtration method is commonly used to treat industrial effluents owing to numerous advantages such as high selectivity, economic and fast operation (Masoudnia et al., 2014). However, membrane filtration method suffer some drawbacks and in order to attain a superior performance in membrane filtration, hybrid process is thus implemented.

1.2 Importance of the Study

This study is useful for reference of future researcher by referring the optimum operating conditions for coagulation using polyaluminium chloride and ultrafiltration membranes. Time can be saved to do research on other factors affecting the coagulation and ultrafiltration. Future work can be improved and knowledge gained by doing this research can be shared among the coagulation and membrane technology field.

1.3 Problem Statement

Malaysia, as one of the developing countries, has experienced high industrial development. With the strategic geographic location, weather and other factors, Malaysia becomes one of the biggest palm oil manufacturers and exporters in the world. MPOC (2012) reported that Malaysia took up 39% of world palm oil production and contributed 44% of world palm oil export. High production rate of palm oil has resulted in the discharge of high amount of effluents. There are about 53 million m³ of palm oil mill effluent (POME) being produced annually in Malaysia (Ujang et al., 2018). Direct discharge of POME into water stream creates a huge impact to both environment and human health. POME containing high solid content deteriorate the quality of clean water and reduces the number of clean water sources for human. Therefore, plenty of treatment methods have been employed to treat POME. Among these treatments, membrane filtration process is found to be more economically feasible and effective in the removal of total suspended solids, turbidity and colour. However, membrane filtration process suffers severe fouling problems in treating POME. Therefore, hybrid process involving coagulation and ultrafiltration is utilized to reduce the fouling problem and to achieve better performance in treatment. Besides, membrane is modified by adding nanoparticles into it to improve the surface properties and increase the rejection of total suspended solids, turbidity and colour for membranes.

1.4 Aim and Objectives

This project was aimed to reduce total suspended solids, turbidity and colour content present in palm oil mill effluent using hybrid coagulation-ultrafiltration process. In order to achieve the overall aim, the objectives of this project are listed as follows:

- i. To determine the optimal operating conditions for coagulation process using polyaluminium chloride (PAC) to remove total suspended solids, turbidity, and colour from anaerobically treated POME.
- ii. To determine the physical properties (cross sectional structure, functional groups, membrane porosity, and pore size distribution) and pure water permeability of fabricated ultrafiltration membranes.
- iii. To determine the effects of TiO_2 loading on permeate flux and reduction of total suspended solids, turbidity and colour for fabricated membranes.
- iv. To investigate the effects of transmembrane pressure on permeate flux and reduction of total suspended solids, turbidity, and colour for fabricated membranes.

1.5 Scope and Limitation of the Study

In this study, hybrid process consists of coagulation and ultrafiltration are used to remove total suspended solids, turbidity and colour from palm oil mill effluent.

The following scope of work is proposed to attain the objectives of this study:

- i. Determine the optimum pH, dosage of coagulant and rapid mixing speed for coagulation process using PAC.
- ii. Fabricate membranes with different compositions of dope solution.
- iii. Characterise the fabricated membrane in terms of surface morphology, pure water permeability, porosity and pore size distribution.
- iv. Determine permeate flux and reduction of total suspended solids, turbidity and colour at different transmembrane pressures.
- v. Determine permeate flux and reduction of total suspended solids, turbidity and colour when using different concentration of TiO_2 in membrane casting.

1.6 Contribution of the Study

Throughout this study, the optimal operating condition for coagulation process using polyaluminium chloride to reduce total suspended solids, turbidity and colour in POME were determined. Several membrane characterization methods and membrane performance test were conducted to determine the optimal concentration of TiO₂ for total suspended solids, turbidity and colour reduction in POME. The correlation between total suspended solids, turbidity and colour were also determined. Future researchers can refer and continue improve findings in this report.

1.7 Outline of the Report

The following chapters include literature review, methodology, results and discussion. Literature review prepares basic knowledge of coagulations using different coagulants, fabrication and characterisation of PES membrane adding titanium dioxide nanoparticles. From the literature review, methodology to conduct research can be determined. After conducting necessary experiments, results will be discussed and analysed.

CHAPTER 2

LITERATURE REVIEW

2.1 Characteristics of Oily Palm Oil Mill Effluent

Palm oil is a vegetable oil that is widely consumed around the world and this increases the production of palm oil significantly. However, voluminous amount of water is required to produce palm oil and therefore huge amount of oily wastewater is created. This oily wastewater is known as palm oil mill effluent (POME).

POME, an effluent which is viscous and consists of large amount of colloidal suspension (Ahmad and Chan, 2009). Raw POME contains large portion of water up to 95 - 96 %, 0.6 – 0.7 % oil and 4 – 5 % total solids (Ahmad et al., 2006). High organic matter content and suspended solids found in POME leads to high turbidity and colour in the solution. POME characteristics are presented in Table 2.1.

Table 2.1: Characteristics of Palm Oil Mill Effluent

Parameters	Concentration*	Units
pH*	4	-
Oil and Grease*	6,000	mg/L
Biochemical Oxygen Demand , BOD ₃ *	25,000	mg/L
Chemical Oxygen Demand, COD*	50,000	mg/L
Total Solids*	40,000	mg/L
Total Suspended Solids*	18,000	mg/L
Volatile Solids*	34,000	mg/L
Ammoniacal Nitrogen*	35	mg/L
Total Nitrogen*	750	mg/L
Turbidity **	11,000	NTU
Colour***	10,000	ADMI

*(MPOB, 2014); ** (Ahmad et al., 2006); *** (Zainal, 2018)

Due to the high concentrations of these contaminants, discharging POME without proper treatment into water is extremely undesirable as it violates the regulations and standards set by the Department of Environment (DOE) Malaysia. Table 2.2 summarises the required standards of different parameters for POME.

Table 2.2: Effluent Standards for Palm Oil Mill (Department of Environment, 2015)

Parameters	Concentration*
pH	5 - 9
Oil and Grease	50
Biochemical Oxygen Demand	100
Chemical Oxygen Demand	-
Total Solids	-
Total Suspended Solids	400
Ammoniacal Nitrogen	100
Total Nitrogen	-
Temperature (°C)	45

By comparing Tables 2.1 and 2.2, it can be clearly seen that untreated POME is unable to be released to the environment. Therefore, proper treatment has to be completed for POME before disposal.

Throughout the past few decades, plenty of methods have been developed to treat POME. Among all the developed methods, biological treatments is commonly used by palm oil mill management to treat POME (Ahmad, Ismail and Bhatia, 2003). It utilizes bacteria to decompose organic matters into different products (Azmi and Yunos, 2014). However, biological treatment system is not ideal due to the high cost and generation of biogas that is corrosive and odorous. Therefore, a combination of coagulation and membrane separation technology is utilized to resolve the problems and challenges in the POME treatment.

2.2 Coagulation as Pre-treatment

Coagulation refers to the chemical process which neutralizes or reduces the electric charge on suspended solids. In the effluent, small particles that have the identical charges causes particles to repel each other, and thus leading to non-settable particles. By introducing coagulants into the effluent, destabilization of colloidal particles is able

to achieve. The neutralization of negative charges introduces Van der Waals force of attraction (Ebeling et al., 2003). As a result, small particles aggregates into microflocs making it easier to be settled and removed.

2.2.1 Colloidal Particles

Palm oil mill effluent is a colloidal suspension which consists of high colloidal particles. These colloidal particles contribute to the high turbidity and colour content in the effluents and are unable to settle themselves. There are several reasons provided by Engelhardt (2010):

- i. Most of the particles have a negative charge causing them to repel each other.
- ii. The force of repulsion is greater than the gravitational force.
- iii. The particles have a very small mass, and thus allowing Brownian motion to interrupt settling.

2.3 Classifications of Coagulants

The types of coagulants are mainly classified into two different groups which are chemical and natural coagulants.

2.3.1 Chemical Coagulants

Chemical coagulants are also referred as inorganic coagulants. It is widely used in the industry due to their attractive price and great performance in treating wastewater. These chemical coagulants are mainly aluminium based and ferrous based. For instance, aluminium sulphate (alum) and polyaluminium chloride (PAC) are aluminium based coagulant whereas ferric chloride and ferric sulphate are ferrous based coagulant. Among these coagulants, alum is frequently selected by the industry to treat different wastewater due to its versatile operating conditions. It provides high effectiveness treatment at room temperature and wide pH ranges (Jagaba et al., 2016). Furthermore, it also assists in charge neutralization as aluminium cation attracts negatively charged particles (Jagaba et al., 2016). Aside from alum, PAC is also utilized by multiple authors to treat different effluent and achieve great performance in coagulation. For instance, PAC was utilized by Bakar and Halim (2013) to remove total suspended solids and chemical oxygen demand (COD) in automotive wastewater.

As a result, PAC achieved 70% removal of COD and 98% of suspended solids. Similarly, PAC was also used by Farajnezhad and Gharbani (2012) to treat effluent from petroleum industry and found out that 81% of total suspended solids were removed.

Besides from aluminium based coagulants, ferrous based coagulants also provide multiple benefits in coagulation process. Flocs produced using ferrous based coagulants tend to be tougher and denser. Moreover, they are to operate in a wider range of pH compared to aluminium based coagulants and are less sensitive to over dosage (Jagaba et al., 2016). However, using inorganic coagulants may arise numerous disadvantages when compared to natural coagulants. For instance, it produces large amount of waste sludge and may affect aquatic organisms due to their toxicity.

2.3.2 Natural Coagulants

Natural coagulants are also known as organic coagulants. Organic coagulants are usually retrieved from plant parts especially the roots, seeds and leaves. Common organic coagulants includes Moringa oleifera, Chitosan, Cicer Aretinum, and Cactus. These organic coagulants are able to achieve a better performance compared to inorganic coagulants when treating wastewater. Most importantly, it is highly biodegradable and does not produce treated water with extreme pH (Jagaba et al., 2016). However, the main drawback for organic coagulants is a much higher pricing compared to inorganic coagulants.

2.4 Conditions Affecting Performance of Coagulation

2.4.1 pH of Solutions

The efficiency of coagulants is highly dependent on the pH of solutions. Therefore, pH adjustment has to be performed before proceeding to coagulation process. Ahmad et al. (2006) found that coagulation using PAC exhibited the highest rejection of total suspended solids at pH 4.5. Using PAC at highly acidic condition causes aluminium cations to exist in significant amount leading to the destabilization of suspended solids. Ahmad, Sumathi and Hameed (2006) also stated that coagulation using PAC at pH higher than 5 decreased the rejection of total suspended solids and turbidity. Besides, Teh et al. (2016) also reviewed that the coagulation performance decreased when coagulation was performed outside the effective pH range due to the re-stabilization of colloids. However, Farajnezhad and Gharbani (2012) reported that the effect of pH

for coagulation was insignificant when PAC was used to treat effluent from petroleum industry.

2.4.2 Dosage of Coagulants

Generally, insufficient or excessive dosage of coagulants will lead to poor performance in coagulation process. Excessive dosage of coagulants causes the agitation of sedimentation process which will result in resuspension of aggregated particles. Similarly, Ahmad, Sumathi and Hameed (2006) also found out that having a higher dosage of coagulant than the optimum amount leads to re-stabilization of colloids which can be observed from the increase of suspended solids reading.

2.4.3 Rapid Mixing Speed

Rapid mixing is an important step in coagulation process which allows the dispersion of coagulants in the solution. Sufficient mixing speed allows high dispersion of coagulants and thus leading to higher effective collision between colloids. Increasing the rapid mixing speed higher than optimum may cause high shear forces in the solution, and thus breaking the flocs formed. However, high shear forces do not always break aggregates but re-organize particles composing flocs, and hence making it more compact (Ahmed et al., n.d.).

2.5 Basics of Membrane Technology

In membrane separation technology, a special porous material that has an interception role is used to remove contaminants physically (Yu, Han and He, 2017). Liquid that flows through the membrane is known as permeate, whilst retentate is the rejected liquid. Membrane is commonly utilized to separate solutes from a solution, but it can also be used for concentrating compounds. Permeate or concentrated retentate stream may be the wanted product depending on the applications and desired product (Juholin, 2016). Table 2.3 shows examples of membrane technology which uses different driving forces.

Table 2.3: Examples of Membrane Processes with Different Driving Force (Juholin, 2016)

Driving Force	Membrane Processes	Separation Mechanism	Typical Separation /Application
Pressure Gradient	Microfiltration	Sieving	Suspended Solids
	Ultrafiltration	Sieving	Colloidal Particles
	Nanofiltration	Sieving, electrostatic interactions, solubility diffusion	Multivalent ions and other charged molecules
	Reverse Osmosis	Differing solubility and diffusion rates of solvent and solutes	Monovalent ions
Thermal Gradient	Membrane Distillation	Evaporation, transport in pores and condensation	Non-volatile compounds from volatile solution
Electrochemical Gradient	Electrodialysis	Differing ionic size, charge and charge density of solute ions	Desalination of water or food, amino acids
Concentration Gradient	Forward osmosis	Diffusion, osmotic pressure	Concentration of streams: activated sludge, anaerobically treated sludge.

Although membrane separation technology involves many different driving forces, the most used membrane technology is pressure driven membrane process (Juholin, 2016). Figure 2.1 illustrates the characteristics of different pressure driven membranes processes.

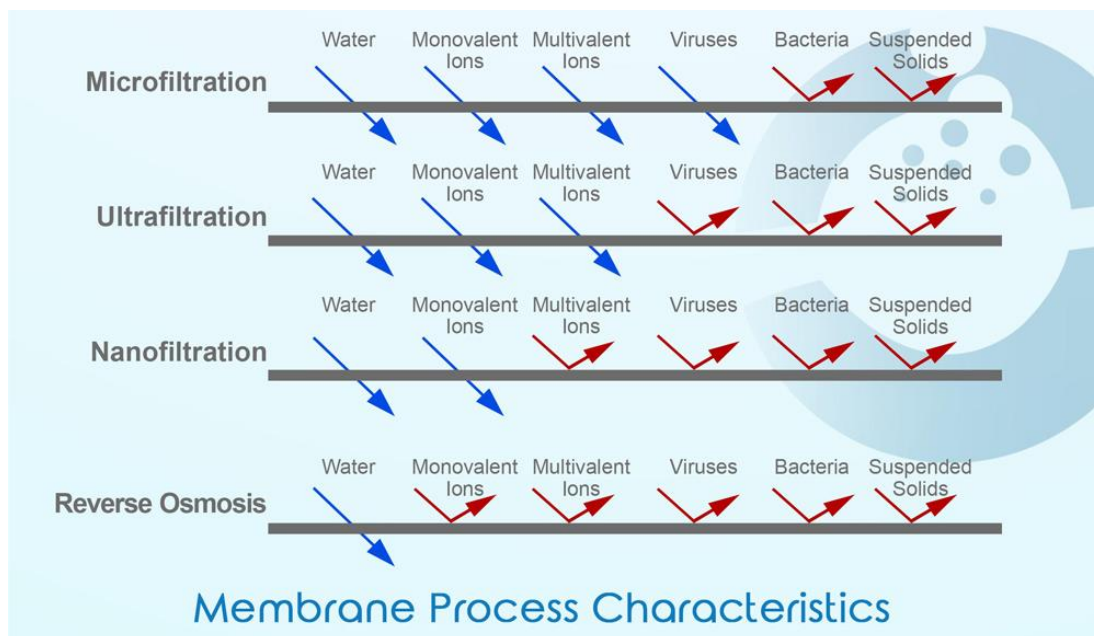


Figure 2.1: Characteristics of Different Pressure Driven Membranes
(OsmotechMembrane, 2018)

Other driving forces of membrane technology are thermal, electrochemical, and concentration gradient. Table 2.4 summarises the advantages and disadvantages for membrane with different driving forces.

Table 2.4: Advantages and Disadvantages for Membrane with Different Driving Forces

Driving Force	Advantages	Disadvantages	References
Pressure Gradient	<ul style="list-style-type: none"> • High selectivity • Easy separation • Economic and fast operation 	<ul style="list-style-type: none"> • Concentration Polarisation • Membrane fouling 	(Masoudnia et al., 2014), (Zhang et al., 2015)
Thermal Gradient	<ul style="list-style-type: none"> • Low operating temperature • Low hydrostatic pressure • Less membrane fouling 	<ul style="list-style-type: none"> • Low permeate flux • High heat loss by conduction • Trapped air within membrane increase mass transfer resistance 	(Alkudhiri, Darwish and Hilal, 2012)
Electrochemical Gradient	<ul style="list-style-type: none"> • High water recovery • Membrane have higher lifespan 	<ul style="list-style-type: none"> • Require additional plumbing and electric controls. 	(Arribas et al., 2015)
Concentration Gradient	<ul style="list-style-type: none"> • external hydraulic pressure for operation are not required • Low membrane fouling problems 	<ul style="list-style-type: none"> • Low permeate flux 	(Terefe et al., 2018)

Pressure driven membranes process studied in this research includes microfiltration, ultrafiltration, nanofiltration and reverse osmosis. Molecules are separated depending on the size of molecules by a sieving effect in microfiltration and ultrafiltration. However, for nanofiltration and reverse osmosis, the separation relies on the interaction of membrane charge with ions.

2.5.1 Microfiltration

Microfiltration membrane pore size typically ranges from 0.1 to 10 μm and this enables microfiltration membrane to separate particles which are larger than 0.1 μm (Jafarinejad, 2017). The operating pressure for microfiltration is between 1 and 2 bar, and thus the energy consumption is relatively lower compared to other membrane technologies (Juholin, 2016). Microfiltration often separates particles that are smaller than the pore size due to the particles adhered on the membrane leading to the

formation of a cake layer (Singh, 2006). Furthermore, the cake layer also assists in reducing the turbidity of permeate (Chon et al. 2014).

2.5.2 Ultrafiltration

Ultrafiltration is capable of eliminating soluble macromolecules from other soluble species. Virus and bacteria are also eliminated using ultrafiltration. The pore size of microfiltration ranges from 0.001 to 0.1 μm and it is operated at a pressure range of 1 – 5 bar (Singh, 2006; Jafarinejad, 2017). Ultrafiltration has a molecular weight cut-off (MWCO) ranging from 1,000 to 500,000 Da (Orecki et al., 2005). Noble and Stern (2003) defined MWCO as “lowest molecular weight of the molecule that is 90% retained by the membrane. Solids and solutes that have high molecular weight are retained in the concentrate, whilst solutes with lower molecular weight passes through the membrane. By using ultrafiltration, particles and microorganisms that may be contaminating the water can be eliminated (Biotech, 2018).

2.5.3 Nanofiltration

By referring to Figure 2.1, nanofiltration is able to separate multivalent ions such as Ni^{2+} , Zn^{2+} , or SO_4^{2-} . Nanofiltration membrane has a pore size of smaller than 2 nm and it operates at a pressure range of 3 – 20 bar (Juholin, 2016; Jafarinejad, 2017). The sieving and charge effects of the membrane lead to the separation in nanofiltration. The membrane will repulse ions that have a similar charge with the membrane, and thus causing the separation to occur (Juholin, 2016). However, nanofiltration requires a higher energy consumption compared to microfiltration and ultrafiltration and it also requires pre-treatment for heavily polluted water.

2.5.4 Reverse Osmosis

Reverse osmosis process uses a semi-permeable membrane which will restrict the flow of particular solutes whilst permitting the flow of solvent. Monovalent ions such as NO_3^- , NO_2^- or NH_4^+ can be separated using reverse osmosis membrane. When the pressure difference is greater than osmosis pressure, reverse osmosis process occurs. This causes water to flow from the concentrated side to the diluted side (Jafarinejad, 2017). The major drawback of reverse osmosis is the high operating pressure which results in high consumption of energy. Besides, oil and grease removal pre-treatment

has to be implemented before the reverse osmosis process due to the fouling susceptibility of membrane by oil.

2.5.5 Hybrid Membrane Process

Hybrid membrane process refers to a membrane separation process that is combined with other processes in order to attain a better separation performance. Hybrid systems tend to reduce the weaknesses of a certain process. Membrane filtration often suffers from membrane fouling problem whereby utilizing hybrid system improves the fouling problem and increases the lifespan of the membrane. Besides, higher removal efficiency can also be achieved through hybrid membrane process (Juholin, 2016). In this study, a hybrid coagulation-ultrafiltration process was utilized to reduce the total suspended solids, turbidity and colour in anaerobically treated POME. Coagulation process was implemented as pre-treatment step before ultrafiltration to reduce total suspended solids, turbidity and colour in the anaerobically treated POME. It allows higher retention of water-soluble substances and contaminants, and thus reducing membrane fouling problem (Ang et al., 2015).

2.6 Membrane Materials

Pressure driven membrane can be made out of numerous types of materials. Commonly, membrane materials can be classified into two groups which are organic and inorganic membranes. Organic membranes are usually polymeric such as Polyvinylidene fluoride (PVDF), Polyethersulfone (PES), Polytetrafluoroethylene (PTFE) and others. Inorganic membranes consist of metallic membranes, ceramic membranes, zeolite membranes and others.

Inorganic membranes possess different strength where it achieves high thermal and chemical stability, has excellent resistance to microbiological resistance and is simpler in cleaning procedure (Synderfiltration, 2018). Due to these astonishing strengths, inorganic membranes have been employed to treat wastewater. However, polymeric membranes are more commonly used as membrane materials due to their lower price compared to inorganic membranes (Juholin, 2016).

For organic membranes, it provides a range of properties that are significant for separation. Although inorganic membranes have a better separation performance than organic membranes, modifications can be made in organic membranes to improve membrane selectivity (Singh, 2006). Therefore, organic membranes are widely used

in industry for separation as they are cost-effective and have satisfactory separation performance.

2.7 Hydrophilicity of Membrane

The characteristics of a membrane are fairly important in order to achieve high performance in treating wastewater. Hydrophilicity is an important characteristic where it can affect the permeate flux and fouling problem in membrane. Hydrophilic membrane (water-attracting) should be used when treating an aqueous feed stream otherwise it could result in severe fouling (Cheryan, 2010). The contact angle test measures the wettability of surface and determines the hydrophilicity of a membrane (Howe and Clark, 2002; Cheryan, 2010). Hydrophilic material causes water droplets to spread out on the surface, resulting in a low contact angle. In contrast, hydrophobic material repels the water and reduces the contact of water with the surface, and thus leading to a high contact angle. Figure 2.2 illustrates the contact angle for both hydrophilic and hydrophobic membranes.

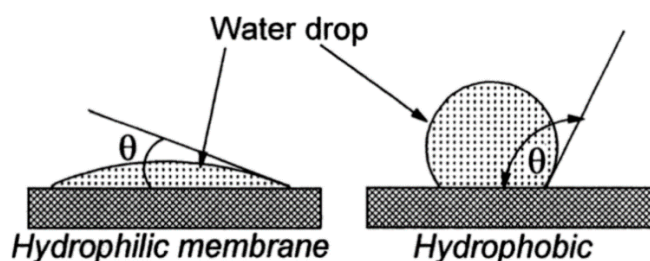


Figure 2.2: Contact Angle for Hydrophilic and Hydrophobic Membranes (Cheryan, 2010)

Hydrophobic membrane tends to attract solids particles to the membrane and causes it to have fouling problems. Unfortunately, many polymeric membranes are hydrophobic in nature and fouling becomes a major drawback in membrane technology (Cheryan, 2010; Juholin, 2016). In order to enhance the performance and reduce fouling problem in membranes, additives such as metal nanoparticles and hydrophilic polymer are added into the membrane for surface modification.

Titanium oxide, TiO_2 nanoparticles are commonly added into polymeric membrane for membrane modification due to its high hydrophilicity, good chemical stability and antibacterial property (Li et al., 2009). It improves the hydrophilicity of polymeric membrane, and thus increasing the flux and mitigating the fouling problem

(Cao et al., 2006). However, Cao et al. (2006) also reported that excessive loading of TiO₂ nanoparticles would weaken the nanometer effect as the nanoparticles aggregate and sediment.

Besides, aluminium oxide, Al₂O₃ nanoparticles can also be used in membrane modification to enhance the hydrophilicity of the membrane. In a studied conducted by Yan et al. (2006), they reported that the addition of Al₂O₃ nanoparticles into PDVF membrane improved the hydrophilicity significantly and therefore increased the permeate flux. However, the permeate flux was unable to increase further when the concentration of Al₂O₃ nanoparticles exceeded a certain limit. Therefore, Yan et al. (2006) concluded that adding 2 wt % of nanoparticles into the membrane would be ideal in terms of economy and practicality.

Furthermore, polyvinylpyrrolidone (PVP) is also frequently used in membrane modification. PVP is a polymer additive that is used to control membrane morphology and to provide hydrophilicity (Kim, Kang and Kim, 2005). In other words, PVP is generally used as a pore former agent that encourages pore formation in the membrane. Ong et al. (2014) conducted a study on PVP and concluded that the porosity, pore size and hydrophilicity were enhanced with the addition of PVP.

2.8 Parameters Affecting the Performance of Membrane Process

2.8.1 Transmembrane Pressure

Transmembrane pressure (TMP) is correlated to permeate flux as TMP is the driving force for the flux. Salahi et al. (2015) defined TMP as “the difference of mean pressure in permeate and retentate channels”. Permeate flux increases linearly with TMP as higher TMP facilitates transport through the membrane (Masoudnia et al., 2014). However, higher TMP forces solid particles to rapidly pass through the membrane pores. This causes membrane fouling to occur more easily as more particles accumulate on the membrane (Masoudnia et al., 2013). Field et al. (1995) introduced the concept of critical flux where the flux depends linearly on TMP when it is below the critical flux. However, when TMP increases beyond the limit, membrane fouling starts to occur and hence reduces the permeate flux. This trend was reported by Hu, Bekassy-Molnar and Koris (2004), where the permeate flux increased linearly at a low TMP and the flux was slightly affected when the operating pressure increased over a critical value. Therefore, an optimum TMP should be applied in order to achieve high permeate flux.

2.8.2 pH of Feed Solution

The pH of the feed solution gives an impact on the permeate flux and membrane fouling problem. Azmi and Yunos (2014) discovered that the permeate flux decreased when the pH of feed solution increased from 5.85 to 7.0. This indicated that the feed chemistry was altered in acidic and basic conditions. Therefore, the pH of the feed solution should be in acidic and basic conditions in order to obtain higher permeate flux. Besides, Mohammadi and Esmaeilifar (2005) discovered that the permeate flux elevated when the feed solution was at basic condition. This is due to the better dissociation of fatty acid molecules in basic condition and hence fatty acids molecules were converted into ions. Hence, the accumulation of fatty acid molecules on the membrane surfaces reduced, and therefore the permeate flux increased (Mohammadi and Esmaeilifar, 2005).

2.8.3 Oil Concentration

The permeate flux is also affected by the concentration of oil in the feed solution. Masoudnia et al. (2014) found that the permeate flux reduced when the oil feed concentration escalated. The high oil concentration caused the thickness gel layer on the membrane surface to increase due to concentration polarization phenomenon (Masoudnia et al., 2014). When the oil feed concentration is low, the hydrodynamic action of the flow was able to eliminate the oil layer formed on the membrane surface and thus not affecting the permeate flux. However, with higher oil feed concentration, the hydrodynamic action of the flow was not capable of removing the oil layer, thus causing the oil layer to increase over time leading to a lower permeate flux. Besides, higher oil feed concentration also caused pore plugging to occur and induced serious membrane fouling problem (Hua et al., 2007).

2.8.4 Temperature of Feed Solution

Permeate flux is also influenced by the temperature of feed solution. Salahi et al. (2011) has revealed that increasing the temperature of feed solution led to the increase of permeate flux. Higher temperature tended to reduce the viscosity of the feed solution, and hence the permeation through the membrane was easier (Sadrazadeh, Gorouhi and Mohammadi, 2008). However, Said et al. (2015) discovered that the permeate flux decreased after the membrane had run for 60 minutes as the membrane was subjected

to irreversible fouling. The deposits on the membrane surface reduced the permeate flux significantly.

2.9 Membrane Fouling

Most of the membrane filtration systems often suffer fouling problem. The fouling problem in membrane filtration system is mainly due to cake formation (Shi et al., 2014). Particles tend to adhere on external surface of membrane, forming a cake layer which increases the resistance to permeate flow. The resistance created by the cake layer is known as cake resistance. However, the initial cake layer formed works as a pre-filter which filters out materials with high fouling potential (Shi et al., 2014). As filtration time increases, more particles reaches the surface of membrane forming a more adhesive cake and resulting in irreversible fouling. The fouling of membrane can be indicated by the decline in permeate flux.

2.10 Cleaning of Fouled Membrane

Membrane fouling greatly affects the permeate flux, and therefore membrane cleaning has to be executed in order to remove the particles that are deposited on the surface of membrane. There are two different cleaning methods which are physical and chemical cleaning method. Chemical cleaning method is more commonly used to clean fouled membrane.

Chemical cleaning agent is applied in chemical cleaning method to remove the particles attached on the surface of membrane and restore the separation characteristics of the membrane. Besides, the chemical cleaning agent is also used to prevent the build-up of new fouling on the membrane surface (Zhao et al., 2000). There are six different categories of chemical cleaning agents. Table 2.5 summarises the types of cleaning agents and their advantages and disadvantages.

Table 2.5: Common Types of Chemical Cleaning Agents with Advantages and Disadvantages (Shi et al., 2014; Regula et al., 2014)

Types	Examples	Advantages	Disadvantages
Acid	Strong: HCl, HNO ₃ Weak: H ₃ PO ₄ , Citric	<ul style="list-style-type: none"> • Precipitates of inorganic salts and metal oxides can be dissolved. • HNO₃ remove organic and biological foulants by nitration 	<ul style="list-style-type: none"> • Strong acids affects pH of solutions and integrity of membrane.
Alkali	Strong: NaOH, KOH Weak: Na ₂ CO ₃	<ul style="list-style-type: none"> • Saponification of fats and oil. • Efficient in neutralising acidic organics. 	<ul style="list-style-type: none"> • Weak bases form insoluble salts with divalent metal ions.
Oxidant	NaClO, H ₂ O ₂ , CH ₃ COCOOH	<ul style="list-style-type: none"> • Remove all pathogenic microorganisms. • Strong cleaner. 	<ul style="list-style-type: none"> • Reduce the lifespan of membrane. • Longer reaction time needed.
Surfactant	Anionic, Cationic, Nonionic	<ul style="list-style-type: none"> • Low rinsing time and consumption of water. • Improve hydrophilicity of membrane. 	<ul style="list-style-type: none"> • Formation of foam during cleaning.
Chelants	EDTA	<ul style="list-style-type: none"> • Effective in destroying cross-linked fouling layer. 	<ul style="list-style-type: none"> • Cleaning efficiency depends on pH.
Enzymes	Proteases, lipases	<ul style="list-style-type: none"> • Prolong membrane lifetime. • Efficient and produce less wastewater. 	<ul style="list-style-type: none"> • Cleaning has to be carried out at optimum temperature for enzymes. • Cost efficiency is difficult to control.

CHAPTER 3

METHODOLOGY AND WORK PLAN

3.1 Methodology Introduction

This research was conducted in two sections for which coagulation was used as pre-treatment. The coagulated POME was used later for membrane filtration to obtain final treated samples. Samples of palm oil mill effluent (POME) were provided by i-Chem Solutions Sdn Bhd, which was obtained from a local palm oil mill located in Sri Jaya, Pahang.

3.1.1 Materials

The main materials required in this study were coagulant, polymeric membranes, dead end filtration unit and palm oil mill effluent (POME). Polyethersulfone (PES) was selected to be the base for polymeric membrane, whereas N-methylpyrrolidinone (NMP) was used as solvent for membrane casting. Besides, additives such as polyvinylpyrrolidone (PVP) and titanium dioxide (TiO_2) were added in membrane dope solution. Table 3.1 summarises the materials required for the experiment with their respective function.

Table 3.1: Materials required for the experiment with their respective function

No.	Material	Function
1	Palm Oil Mill Effluent	Wastewater sample
2	Polyaluminium Chloride (PAC)	Coagulant
3	Concentrated HCl (37 w/w %)	pH adjuster
4	Sodium Hydroxide Pellets	pH adjuster
5	Polyethersulfone (PES)	Membrane polymer
6	N-methylpyrrolidinone (NMP)	Membrane solvent
7	Titanium Dioxide (TiO_2)	Additive, nanoparticle
8	Polyvinylpyrrolidone (PVP)	Additive, pore former

3.2 Coagulation using Polyaluminium Chloride (PAC)

Palm Oil Mill Effluent (POME) was subjected to coagulation process using polyaluminium chloride (PAC) as coagulant prior to membrane filtration process. The coagulation process was carried out using a flocculation test unit (LS-260001-A) involving 4 working gang stirrers as shown in Figure 3.1. The pH of POME solution was first adjusted using concentrated HCl or sodium hydroxide. PAC was then added into the pH-adjusted POME for coagulation. The mixing of POME solution was carried out using rapid mix and slower mix. Durations for rapid mix and slower mix were fixed at 1 and 30 minutes, respectively. The coagulated samples were removed from the flocculation test unit and allowed to settle for 60 minutes. The pH, coagulant dosage and rapid mixing speed were optimized for the best reduction of total suspended solids, turbidity and colour from the anaerobically treated POME.



Figure 3.1: Flocculation Test Unit (LS-260001-A)

3.2.1 Optimum Coagulant Dosage

The pH of POME solution and rapid mixing speed were fixed at 4.5 and 150 rpm, respectively. Different dosages of PAC were added into the POME solution ranges from 200 to 1000 mg/L. Total suspended solids, turbidity and colour for coagulated samples were determined to obtain optimum coagulant dosage for the coagulation process.

3.2.2 Optimum pH

The optimum pH for coagulation process was obtained via optimum coagulant dosage. Similarly, the rapid mixing speed was set at 150 rpm in the coagulation process. The pH for POME solution was varied from acidic to alkaline range (2.0 – 9.0). Likewise, total suspended solids, turbidity and colour for coagulated samples were determined to obtain optimum pH for the coagulation process.

3.2.3 Optimum Rapid Mixing Speed

The optimum rapid mixing speed was determined using optimum coagulant dosage and optimum pH. The rapid mixing speed of coagulation process was varied from 100 to 250 rpm. Identically, total suspended solids, turbidity and colour for coagulated samples were determined to obtain optimum rapid mixing speed for the coagulation process.

3.3 Membrane Fabrication

3.3.1 Dope Solution Preparation

In this study, different compositions of dope solution were prepared for the fabrication of ultrafiltration (UF) membranes. Table 3.2 summarises different compositions of dope solution.

Table 3.2: Compositions of Dope Solution for Ultrafiltration Membranes

No.	Membrane ID	Composition (weight %)			
		PES	TiO ₂	PVP	NMP
1	U1	16.0	-	1.0	83.0
2	U2	16.0	0.1	1.0	82.9
3	U3	16.0	0.5	1.0	82.5
4	U4	16.0	1.0	1.0	82.0

Based on Table 3.2, 4 sets of different dope solution were used to cast the membranes. The PES composition for all UF membrane were set at 16 % with 1 % of PVP. Different amounts of TiO₂ nanoparticles were added into U2 – U4. NMP solvent took up the rest of the composition percentage. U1 was the control set for this

experiment to compare the performance between U2 to reveal the difference between both membranes in the presence of TiO_2 .

Before casting a membrane, a homogenous dope solution was obtained by mixing different doping materials. Moisture content in PES pellets was first removed by drying it using an oven at 60°C for 24 hours. Then, PES pellets were added into the NMP solvent and stirred at the speed of 600 rpm until all the pellets were dissolved. Pre-weighted TiO_2 nanoparticles and PVP were added to produce the dope solution. The dope solution was sonicated using an ultrasonic cleaner (SK5200GT, KUDOS) as shown in Figure 3.2 to ensure all the additives were completely dispersed in the dope solution and to remove any additional air bubbles in the dope solution.



Figure 3.2: Ultrasonic Cleaner (SK5200GT, KUDOS)

3.3.2 Membrane Casting

Phase inversion technique was used to prepare all the membrane. Firstly, the dope solution was applied onto a clean and smooth glass plate. Then, a hand casting knife was used to spread the dope solution evenly on glass plate. The casting thickness of the membrane was $250\ \mu\text{m}$. The glass plate was placed into a distilled water bath to allow the formation of membrane through solvent-nonsolvent exchange.

3.4 Characterizations of Membranes

3.4.1 Membrane Porosity

The porosity of the membranes was calculated using Equation 3.1. Both wet and dry weights of the membrane were needed to calculate the membrane porosity. The wet weight of the membrane was measured using an analytical weight balance, whereas the dry weight was measured by drying the membrane for 24 hours at 40 °C. The average values were obtained by repeating the procedures for 3 times for each sample.

$$E = \frac{\frac{w_w - w_d}{\rho_w}}{\frac{(w_w - w_d)}{\rho_w} + \frac{w_d}{\rho_m}} \quad (3.1)$$

where

ε = porosity of membrane

w_w = wet weight of membrane, g

w_d = dry weight of membrane, g

ρ_w = density of water, g/cm³

ρ_m = density of membrane, g/cm³

3.4.2 Pore Size Distribution

The pore size distribution of the membranes was determined using Equation 3.2.

$$r_m = \sqrt{\frac{(2.9 - 1.75\varepsilon)8\eta l Q}{\varepsilon A \Delta P}} \quad (3.2)$$

where

r_m = average pore size, m

ε = porosity of membrane

η = water viscosity at 25 °C, Pa·s

l = membrane thickness, m

Q = volume of the permeate water per unit time, m³/h

A = effective area of the membrane, m²

ΔP = operational pressure, Pa

3.4.3 Scanning Electron Microscopy (SEM) Analysis and Energy-dispersive X-ray Spectroscopy (EDX) Analysis

Scanning electron microscopy (SEM) was used view the surface and cross sectional morphology of the membranes. Prior to the analysis, the membrane was first immersed into liquid nitrogen for freeze fracturing to acquire a clean cut cross section. The cross section of the sample was coated with a layer of gold or platinum using a sputter coater and the morphology structures were examined using SEM. Figures 3.3 and 3.4 illustrate SEM (S-3400N, Hitachi) and sputter coater (SC7620, EMITECH), respectively.



Figure 3.3: Scanning Electron Microscopy (S-3400N, Hitachi)

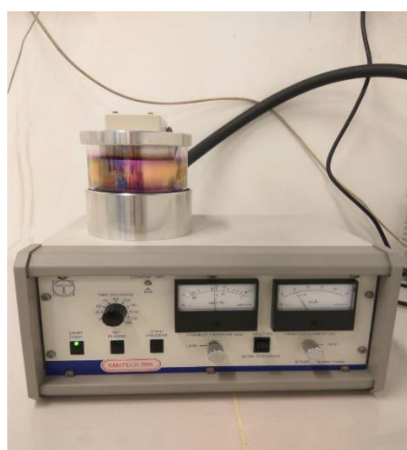


Figure 3.4: Sputter Coater (SC7620, EMITECH)

Energy-dispersive X-ray Spectroscopy (EDX) was used to determine the components that exist in all the fabricated membranes. The existence of TiO_2 on the surface of membranes was studied using EDX.

3.4.4 Fourier Transform Infrared Spectroscopy (FTIR)

Fourier Transform Infrared (FTIR) spectroscopy was used to identify the functional groups on the fabricated membranes. The sample holder was first disinfected using alcohol to obtain the background spectrum. Then, the sample was placed onto the specimen holder to run the analysis. The functional groups for the fabricated membranes was determined by different wavenumber. Figure 3.5 illustrates the FTIR instrument (IS10, NICOLET).

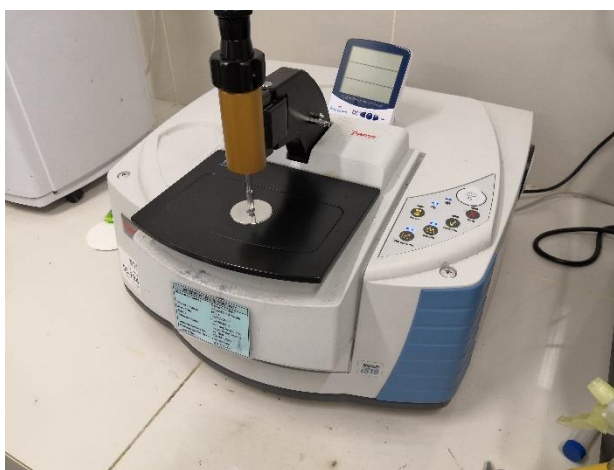


Figure 3.5: FTIR Instrument (IS10, NICOLET)

3.4.5 Pure Water Permeability

Permeability of the fabricated membranes was measured using pure water permeability. The fabricated membrane was placed into a dead end filtration column and 300 mL of distilled water was fed into the column. The system was pressurized to allow permeate to pass through the membrane. The volume of permeate and the sampling time were measured and Equation 3.3 was used to calculate the pure water flux.

$$J_w = \frac{V}{A \times \Delta t} \quad (3.3)$$

where

J_w = Pure water flux, L/ (m².h)

V = Volume of distilled water, L

A = Effective membrane area, m²

Δt = Sampling time, h

3.5 Membrane Filtration

3.5.1 Experimental Setup

A dead end filtration unit was required in this study. The experimental setup consisted of a nitrogen (N_2) cylinder tank, a pressure gauge, a stirred cell with a magnetic stirrer and an electronic balance. The system was pressurized using N_2 gas and the feed solution was continuously injected into the stirrer cell to produce permeate. Permeate flux was measured gravimetrically using an electronic balance. Figure 3.6 shows the schematic diagram of the experimental setup. The transmembrane pressure (TMP) was varied in this experiment and the permeate flux was calculated.

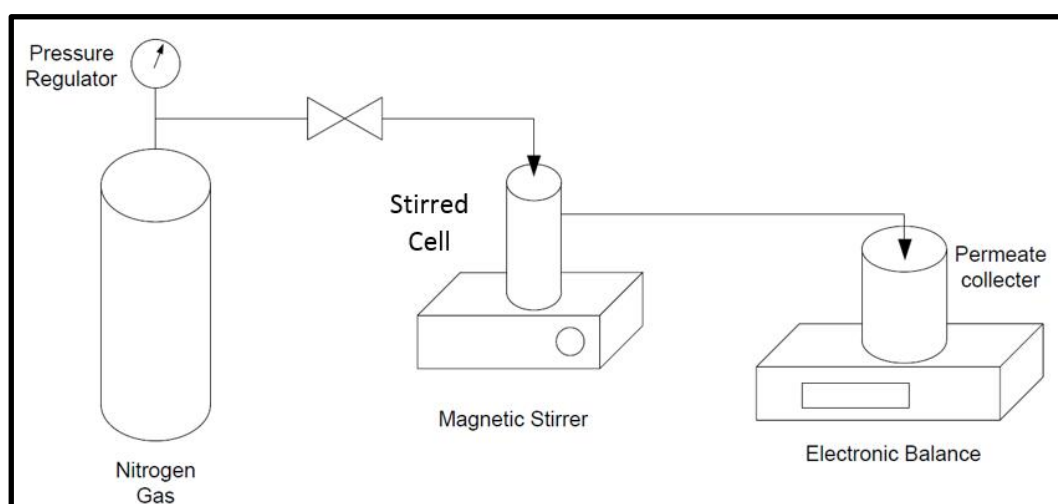


Figure 3.6: Schematic Diagram of Dead End Filtration System

3.5.2 Transmembrane Pressure

The fabricated membranes were subjected to different transmembrane pressures (TMP) to investigate the effect of TMP on permeate flux and reduction of total suspended solids, turbidity and colour. The coagulated samples were fed into the dead end filtration unit and the pressure for ultrafiltration process was varied from 2 to 5 bar. The permeate flux was measured and the total suspended solids, turbidity and colour of filtered samples were determined to obtain an optimum TMP for the ultrafiltration process.

3.5.3 Permeate Flux

The permeate flux was determined using Equation 3.4 which is identical to the pure water permeability.

$$J_w = \frac{V}{A \times \Delta t} \quad (3.4)$$

where

J_w = Permeate flux, L/ (m².h)

V = Volume of permeates, L

A = Effective membrane area, m²

Δt = Sampling time, h

3.6 Determination of Total Suspended Solids

The total suspended solids of all coagulated samples and membrane filtered products were determined using a spectrophotometer (HACH DR 3900) as shown in Figure 3.7. The spectrophotometer was operated based on photometric method 8006 provided by HACH. The total suspended solids for untreated POME, coagulated POME and membrane filtered POME was determined to evaluate the percentage of reduction.

The percentage of reduction was calculated using Equation 3.5:

$$R = \left(1 - \frac{C_p}{C_f}\right) \times 100\% \quad (3.5)$$

where

R = Percentage of reduction (%)

C_p = Concentration in permeate, mg/L

C_f = Concentration in feed solution, mg/L

3.7 Determination of Colour

The determination of colour was also carried out using a spectrophotometer (HACH DR 3900). The colour of solutions were measured in American Dye Manufacturers Institute (ADMI) unit and the spectrophotometer was operated based on Method 10048 provided by HACH. Similarly, the colour for untreated POME, coagulated POME and membrane filtered POME were measured for the evaluation of percentage of reduction. The percentage of colour reduction was evaluated using Equation 3.6.

$$R = \left(1 - \frac{C_p}{C_f}\right) \times 100\% \quad (3.6)$$

where

R = Percentage of reduction (%)

C_p = Colour in permeate, ADMI

C_f = Colour in feed solution, ADMI



Figure 3.7: HACH DR 3900 Spectrophotometer

3.8 Determination of Turbidity

The turbidity of different POME samples was measured using a turbidity meter (TN-100, Eutech Instruments) in Nephelometric Turbidity Units (NTU) as shown in Figure 3.8. The turbidity for untreated POME, coagulated POME and membrane filtered POME were measured to calculate the percentage of reduction. The percentage of reduction was evaluated using Equation 3.7.

$$R = \left(1 - \frac{C_p}{C_f}\right) \times 100\% \quad (3.7)$$

where

R = Percentage of reduction (%)

C_p = Turbidity in permeate, NTU

C_f = Turbidity in feed solution, NTU



Figure 3.8: Turbidity Meter (TN-100, Eutech Instruments)

CHAPTER 4

RESULTS AND DISCUSSION

4.1 Optimization of Operating Conditions for Coagulation Process

4.1.1 Optimum pH condition

Coagulation process is highly sensitive to the pH condition of solutions. Based on Figure 4.1, the percent reduction of total suspended solids, turbidity and colour achieved the highest at pH 4. The percent reduction of total suspended solids, turbidity and colour at pH 4 were 99.67%, 92.19% and 93.85%, respectively. It could be observed that PAC had a better performance when it was subjected to acidic condition as the reduction of turbidity and colour were slightly higher. The results were consistent with the finding from Ahmad et al. (2006). The addition of acid reduces the surface charges, and hence eliminating the inter-particle forces and promoting electrostatic attraction which enhanced the destabilization of colloid particles (Teh et al., 2016). For aluminium based coagulant, high amount of positively charge aluminium cation exists in lower pH effluent which creates a favourable condition for charge neutralization to occur (Teh et al., 2016). However, the performance of PAC in reduction of turbidity and colour decreased significantly when the pH of POME was set at 5 and above. This might due to the re-stabilization of colloids particles as the coagulation process was conducted beyond effective pH range.

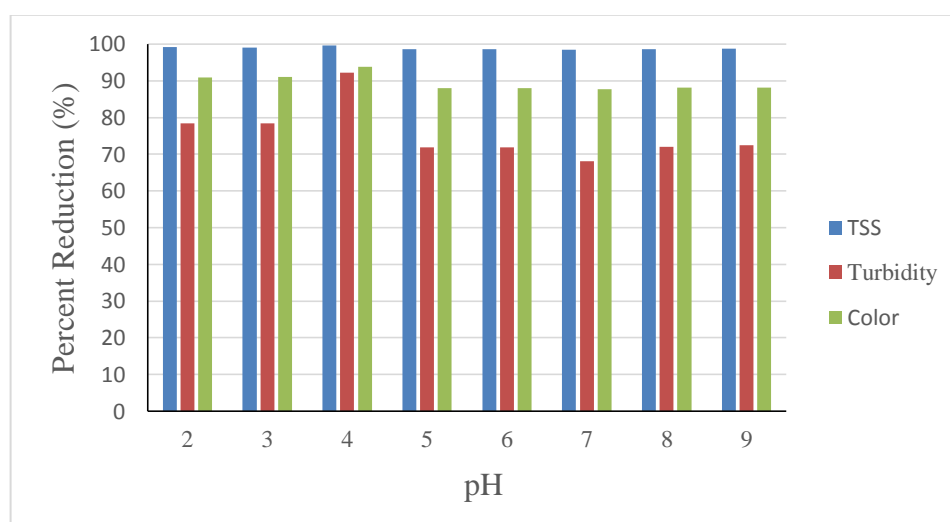


Figure 4.1: Percent Reduction for Total Suspended Solids, Turbidity and Colour at different pH under 600 mg/L coagulant dosage and 150 rpm rapid mixing speed

4.1.2 Optimum PAC Dosage

The dosage of coagulant is a critical factor for the performance and cost of coagulation process. Excessive dosage of coagulant results in higher cost of treatment and reduces performance of coagulation process. The process is said to be overdosed when it reaches the critical coagulation concentration where there exists an inflection point in the reduction performance (Teh et al., 2016). Based on Figure 4.2, it was observed that the reduction of total suspended solids (TSS) at different dosages of coagulants achieved a high percentage reduction up to 99.78%. The reduction efficiencies of turbidity and colour were the highest at the coagulant dosage of 600 mg/L. Thus, it could be deduced that the optimum dosage of PAC at the condition of pH 4 and 150 rpm rapid mixing speed was at 600 mg/L. At the coagulant dosage lower than 600 mg/L, the percent reduction of, turbidity and colour were significantly lower due to the insufficient amount of coagulant present in POME. Inadequate of adsorption sites in coagulant restricted bridge formation between adjacent particles resulting in re-stabilization of colloid particles (Teh et al., 2014). For PAC dosage greater than 600 mg/L, the coagulant dosage was said to be applied beyond the critical coagulation concentration point as the reduction efficiencies of turbidity and colour were slightly lower compared to that of optimum dosage. High amount of PAC might lead to the re-stabilization of counter ion, resulting in the dispersion of flocs thus restricting the settling of particles (Norulaini et al., 2001).

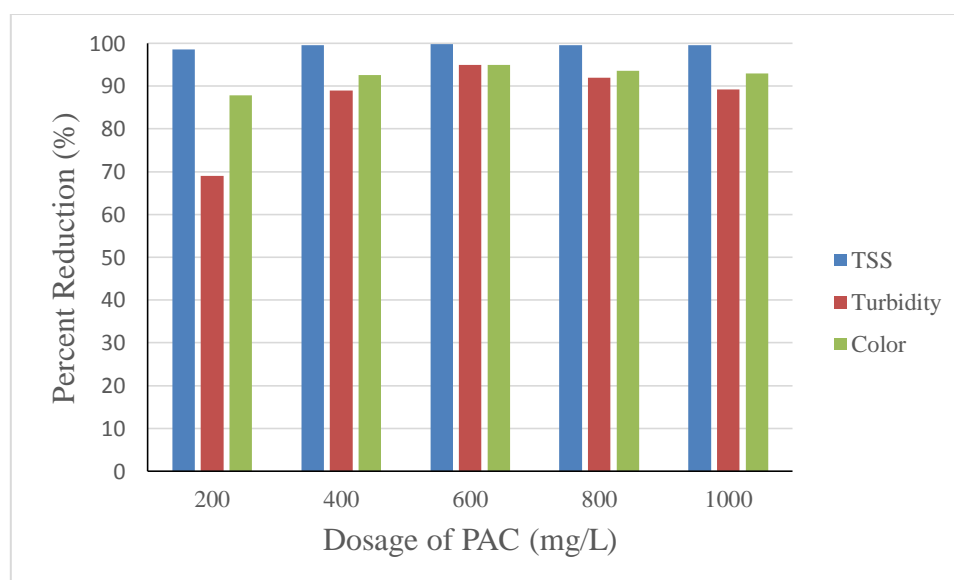


Figure 4.2: Percent Reduction for Total Suspended Solids, Turbidity and Colour at Different Coagulant Dosage under pH 4 and 150 rpm Rapid Mixing Speed

4.1.3 Optimum Rapid Mixing Speed

Rapid mixing speed has a great impact on the coagulation process where the success of the process highly depends on it. Based on Figure 4.3, the percent reduction of TSS, turbidity and colour were found to be the highest under 200 rpm of rapid mixing speed at the condition of pH 4 and 600 mg/L coagulant dosage. The percent reduction for TSS, turbidity and colour were 99.74%, 94.44% and 94.60%, respectively. The performance of coagulation process decreased when the rapid mixing speed was lower than 200 rpm. Lower rapid mixing speed offered a lower particle collision rate, and thus decreasing the flocs formation rates and resulting in poorer performance of coagulation process. Besides, rapid mixing speed above 200 rpm also experienced a slight drop in percent reduction. Generation of high shear force due to high rapid mixing speed caused primary particles forming the flocs to be unable to aggregate. Therefore, flocs were unable to form at high rapid mixing speed.

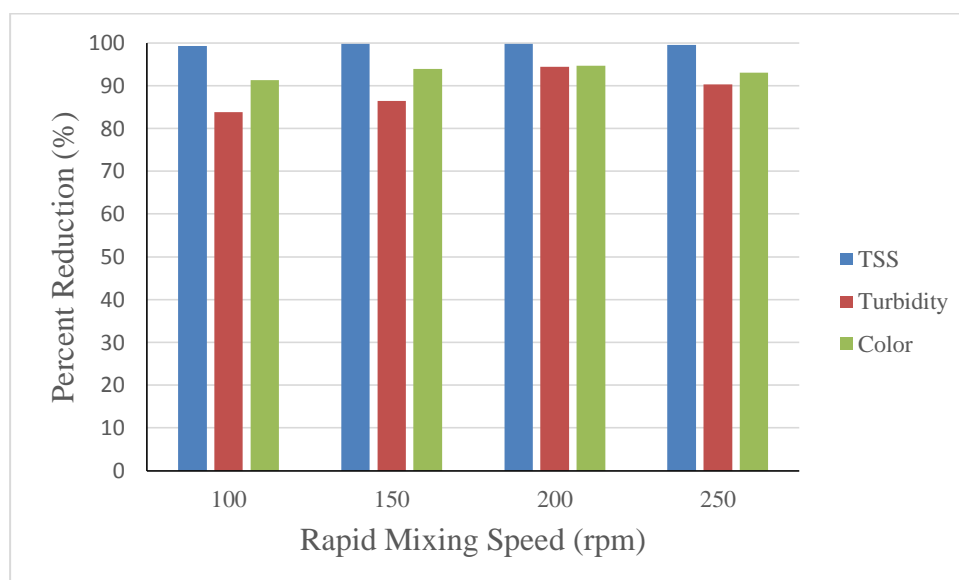


Figure 4.3: Percent Reduction for Total Suspended Solids, Turbidity and Colour at Different Rapid Mixing Speed under pH 4 and 600 mg/L Coagulant Dosage

4.2 Characterization of Fabricated Membranes

4.2.1 Cross-Sectional Morphology

Figure 4.4 illustrates the cross-sectional structure for all 4 different membranes which were U1, U2, U3 and U4. Generally, a dense top layer and porous support layer were noticed in all fabricated membranes. Membrane U1 formed a denser membrane structure when compared to other membranes. This was due to the slower diffusion

rate between solvent to non-solvent. Dope solution without nanoparticles created a stronger affinity, leading to a lower demixing (solidification) rate. Therefore, membrane U1 showed a more compact structure in the top layer due to slower phase inversion process.

For membranes U2, U3 and U4, TiO₂ nanoparticles were added to modify the morphology of the membrane. The addition of TiO₂ nanoparticles increased mass transfer during the phase inversion process as it provided a high specific area and good hydrophilicity (Li et al., 2009). Membranes U2 to U4 showed an increasing size of finger-like macrovoid structure due to due to higher diffusion rate of dope solution in the phase inversion stage. The higher loading of TiO₂ nanoparticles caused the pore size and porosity to increase which eventually increased the pure water permeability of membranes (as discussed in Section 4.2.4).

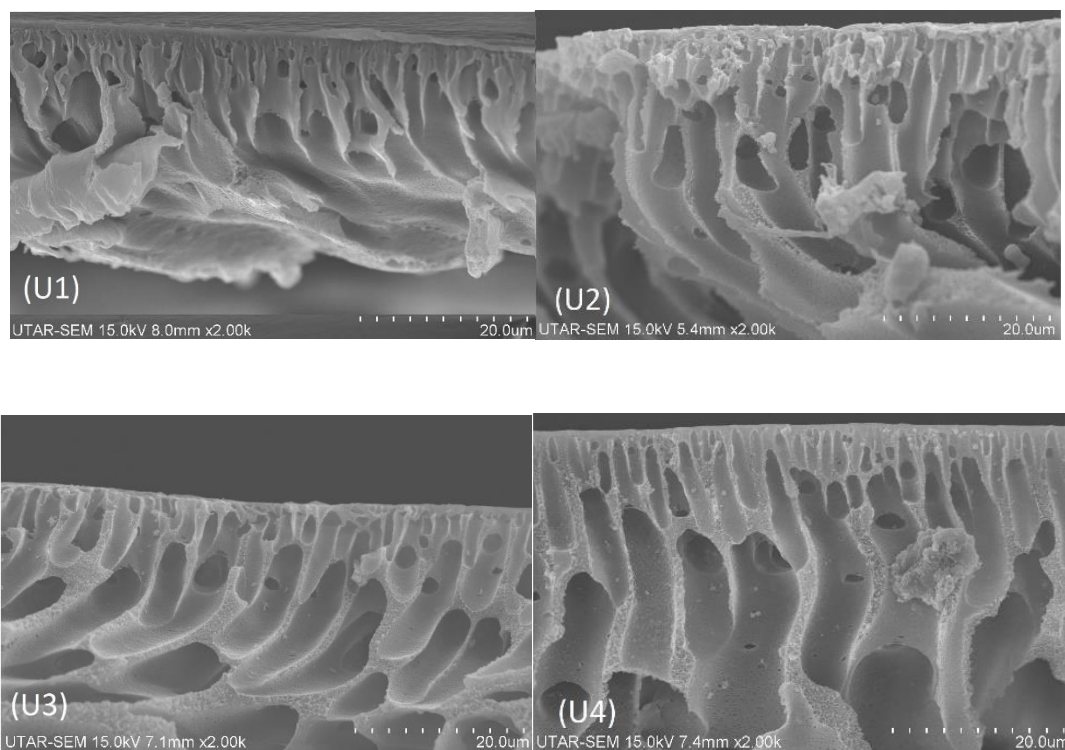


Figure 4.4: SEM Micrographs of Cross-Sectional Structure for Membranes U1, U2, U3 and U4 at Magnification of 2000x

4.2.2 Fourier Transform Infrared Spectroscopy (FTIR) Results

The FTIR analysis of 4 different membranes is demonstrated in Figure 4.5. The spectrum of 4 FTIR showed the characteristics peak of PES molecular structure. PES structure consists of a benzene ring, an ether bond, and sulfone structure (Qu et al., 2010). The C-H stretching peak could be observed at 3086 cm^{-1} . The aromatic skeletal vibration was shown by three different peaks between 1400 and 1600 cm^{-1} . The peak situated at 1100 cm^{-1} showed the S=O stretching peak.

FTIR analysis was performed on both membranes U1 and U2 to compare the changes of bandwidth brought by the addition of TiO_2 nanoparticles.

It was observed that there was no alteration of peak when nanoparticles were added. Therefore, it could be deduced the addition of TiO_2 nanoparticles did not change the bonds and functional groups formed in the membranes.

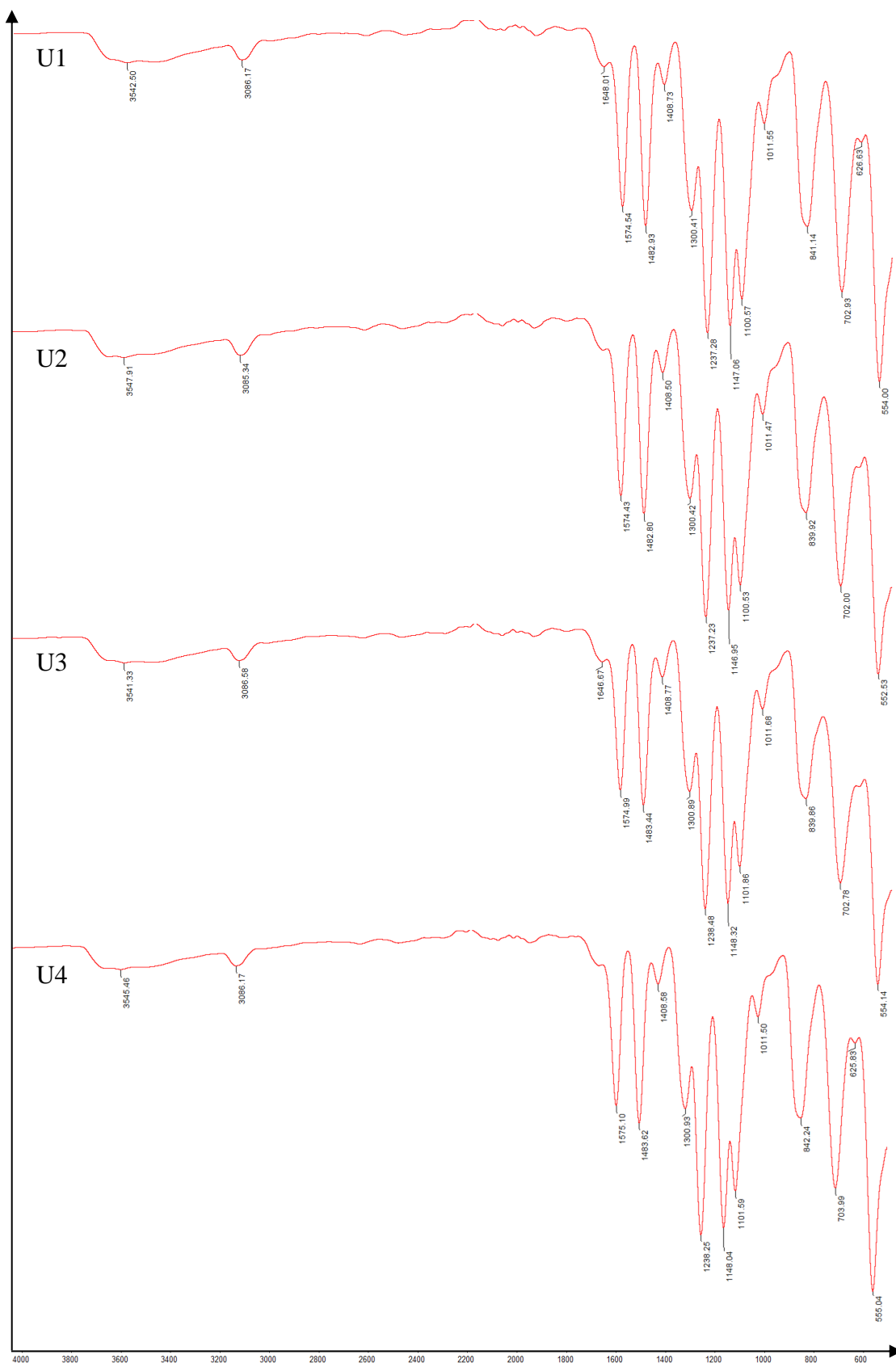


Figure 4.5: FTIR Spectrum for Different Types of Membranes

4.2.3 Energy Dispersive X-ray Spectroscopy (EDX)

Based on Tables 4.1 and 4.2, it could be seen that the TiO₂ nanoparticles were successfully incorporated into the membrane matrix and the amount of nanoparticles increased across the membranes. The chemical composition of polyethersulfone (PES) contributed to the presence of carbon (C), oxygen (O) and sulphur (S) composition in the matrix of membranes.

Table 4.1: Weight Percent (wt%) of Membranes

	U1	U2	U3	U4
	Weight Percent (wt%)			
C	61.16	62.08	60.19	57.05
O	29.70	22.56	30.65	22.96
S	9.14	14.89	8.51	16.19
Ti	0.00	0.46	0.65	3.80

Table 4.2: Atomic Percent (At%) of Membranes

	U1	U2	U3	U4
	Atomic Percent (At%)			
C	70.40	73.28	69.54	70.17
O	25.66	20.00	26.59	21.20
S	3.94	6.59	3.68	7.46
Ti	0.00	0.14	0.19	1.17

4.2.4 Porosity and Pore Size Distribution Results

The membrane was highly affected by the diffusion rate of solvent in the phase inversion stage. Based on Table 4.3, it was observed that the porosity of membranes increased from membranes U1 to U4. By comparing membranes U1 and U2, the porosity of membrane U2 increased owing to the addition of TiO₂ nanoparticles. Membrane U4 with the highest amount of TiO₂ possessed the highest porosity of 0.8958. The hydrophilic properties of TiO₂ accelerated the diffusion rate between solvent and non-solvent, and thus promoting the membrane formation. Therefore, the addition of TiO₂ nanoparticles improved the porosity of membranes.

The pore size of membranes is also tabulated in Table 4.3. As the loading of TiO₂ increased, the pore size of membranes also increased. Membrane U4 exhibited the largest pore size among other membranes due to the highest amount of nanoparticles added. The addition of nanoparticles reduced the affinity of dope solution causing faster demixing (solification) to occur, and eventually resulting in large pore size. A strong affinity led to delayed demixing, and formation of smaller pore size (Thuyavan et al., 2016).

Table 4.3: Porosity and Pore Size of Membranes

Membrane	Porosity (%)	Pore size (μm)
U1	85.26	0.071
U2	87.67	0.076
U3	89.26	0.082
U4	89.58	0.091

4.2.5 Pure Water Permeability Results

Figure 4.6 presents the pure water permeability results for different membranes. The pure water permeability of membranes was observed to demonstrate an increasing trend with the higher amount TiO₂ nanoparticles added into the membranes. The addition of TiO₂ nanoparticles increased the pore size and porosity of membranes, and therefore promoting the permeation of water. However, low amount of TiO₂ nanoparticles might have insignificant effect to the pure water permeability of membrane as depicted by membrane U2. The addition of 0.1% of TiO₂, however, did not promote the pure water permeability of membrane, but it was shown to have a relatively higher pure water permeability in membranes U3 and U4 due to higher amount of TiO₂ nanoparticles added.

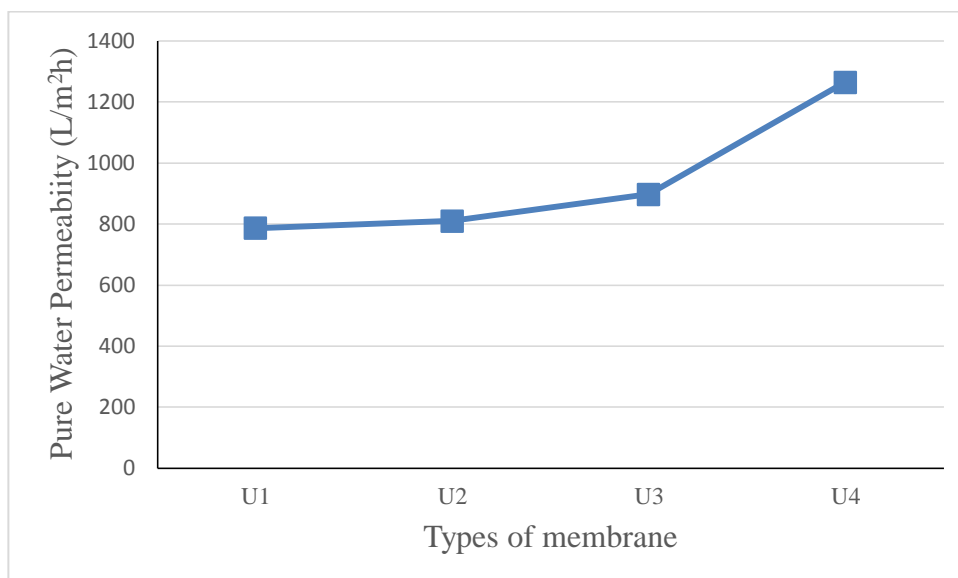


Figure 4.6: Pure Water Permeability of Membranes under Transmembrane Pressure of 1 bar

4.3 Membrane Filtration Results

4.3.1 Effect of TiO₂ Loading on Permeate Flux

As mentioned earlier, the addition of TiO₂ nanoparticles into PES membrane increased its hydrophilicity. Therefore, a higher concentration of TiO₂ in a membrane would provide a higher permeate flux. The permeate flux for different membranes under TMP of 3 bar is presented in Figure 4.7. It was observed that the permeate flux increased across membranes as the concentration of TiO₂ nanoparticles increased. This finding was found to be consistent with the pure water permeability of the membranes illustrated in Figure 4.6, where the pure water permeability of membranes increased with the concentration of TiO₂ nanoparticles.

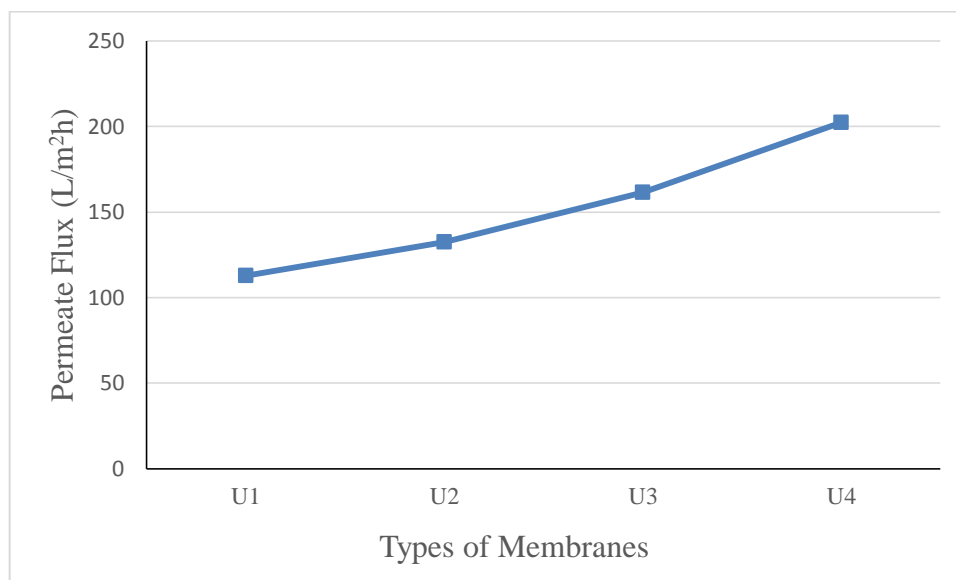


Figure 4.7: Permeate Flux for Different Types of Membranes under Transmembrane Pressure of 3 bar

4.3.2 Effect of TiO₂ Loading on Reduction of Total Suspended Solids, Turbidity and Colour

Based on Figure 4.8, U4 had the highest percent reduction of TSS, turbidity and colour. The percent reduction of TSS, turbidity and colour were 78%, 85.81% and 74.12%, respectively. However, the effects of TiO₂ loading on reduction of TSS, turbidity and colour were studied by comparing the reduction by other membranes. It was observed that the percent reduction by other membranes did not show any significant changes, indicating that the increased loading of TiO₂ did not give a higher reduction in TSS, turbidity and colour. The addition of low TiO₂ nanoparticles concentration in membrane might result in insignificant effect in the reduction of TSS, turbidity and colour. Therefore, a higher concentration of TiO₂ should be added into the membrane in order to study determine effect in reduction of TSS, turbidity and colour. Hence, it could be concluded that the addition of low TiO₂ concentration only increased permeate flux, but not improve the reduction of TSS, turbidity and colour, although surface modification was made.

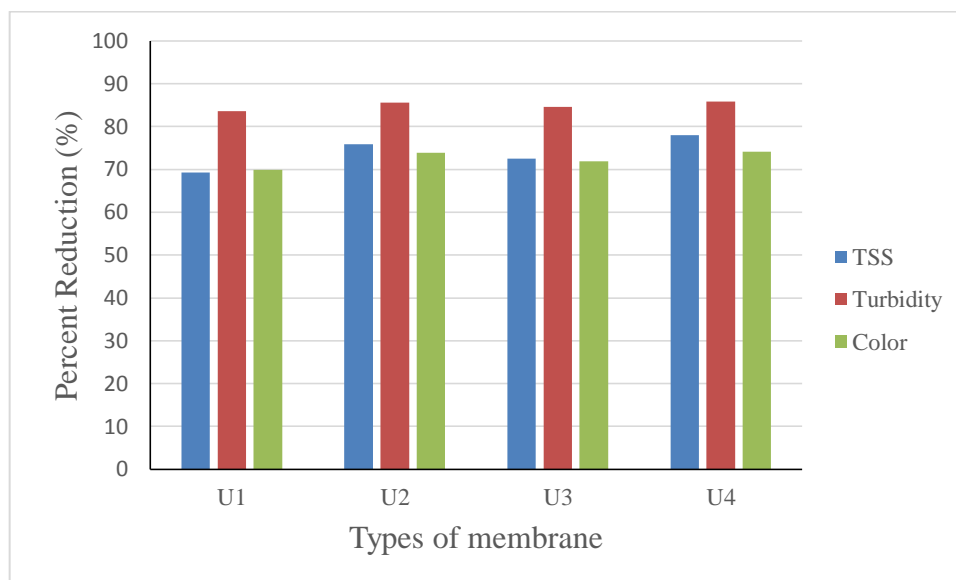


Figure 4.8: Percent Reduction of Total Suspended Solids, Turbidity and Colour for Different Types of Membranes under Transmembrane Pressure of 3 bar

4.3.3 Effect of Transmembrane Pressure on Permeate Flux

Figure 4.9 depicts the permeate flux for membrane U3 at different TMPs. The results showed that the permeate flux for the membrane increased accordingly with higher TMP. TMP is the driving force for the permeate flux. With higher TMP, higher forces were exerted onto the membrane to allow the flux to increase. Therefore, it could be summarized that that higher TMP would give a greater permeate flux. However, TMP applied onto the membrane should not exceed the mechanical strength of membrane which would cause rupture of membrane, leading to low separation efficiency.

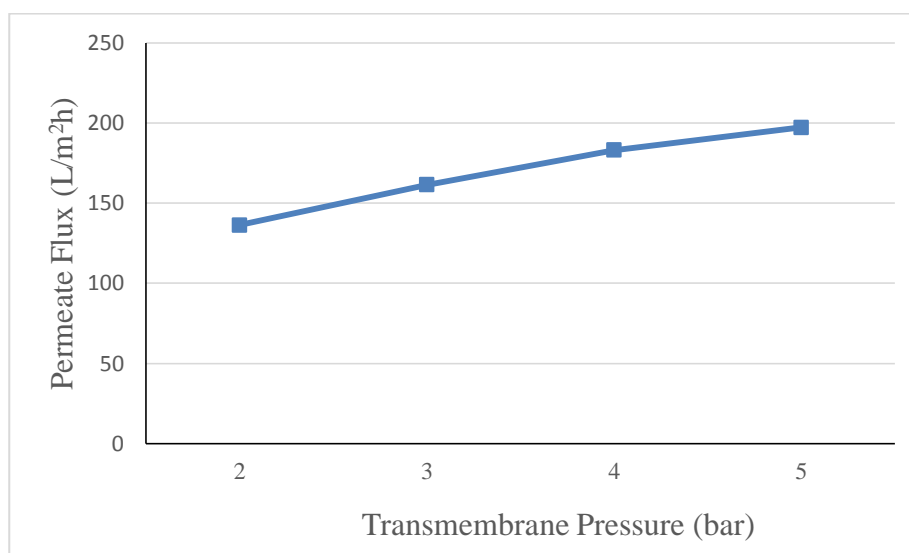


Figure 4.9: Permeate Flux for Membrane U3 at Different Transmembrane Pressures

4.3.4 Effect of Transmembrane Pressure on Reduction of Total Suspended Solids, Turbidity and Colour

Based on Figure 4.10, the reduction of TSS, turbidity and colour presented an increasing trend and decreases after applying TMP of 4 bar. It was found that the optimum TMP for the reduction of TSS, turbidity and colour for membrane U4 was at 3 bar as it achieved the highest percent reduction. The percent reduction for TSS, turbidity and colour were 78.02%, 85.81% and 74.12%, respectively. It was observed that applying TMP greater than 4 bar experienced a significant drop in percent reduction. This was due to the high TMP force exerted onto the membrane causing solid particles to rapidly pass through the membrane, and hence creating a lower percent reduction. Greater TMP caused more particles to force through the membrane without separation, leading to even lower percent reduction. This can be seen from the percent reduction TMP of 5 bar as it had a lower percent reduction compared to that at TMP of 4 bar. The same results were achieved using membrane U1, U2 and U3 which were depicted in Figures 4.11, 4.12, and 4.13, respectively.

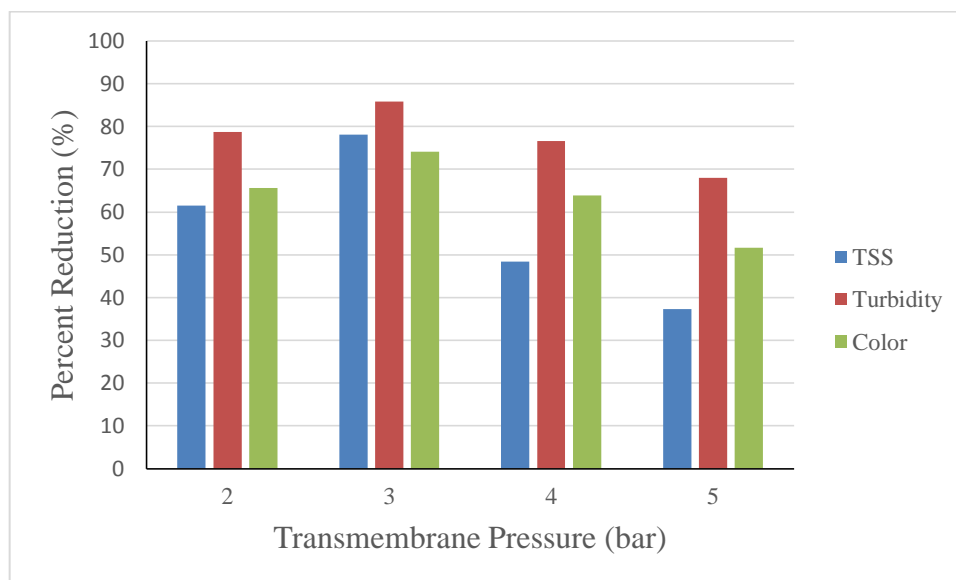


Figure 4.10: Percent Reduction of Total Suspended Solids, Turbidity and Colour for Membrane U4 under Different Transmembrane Pressures

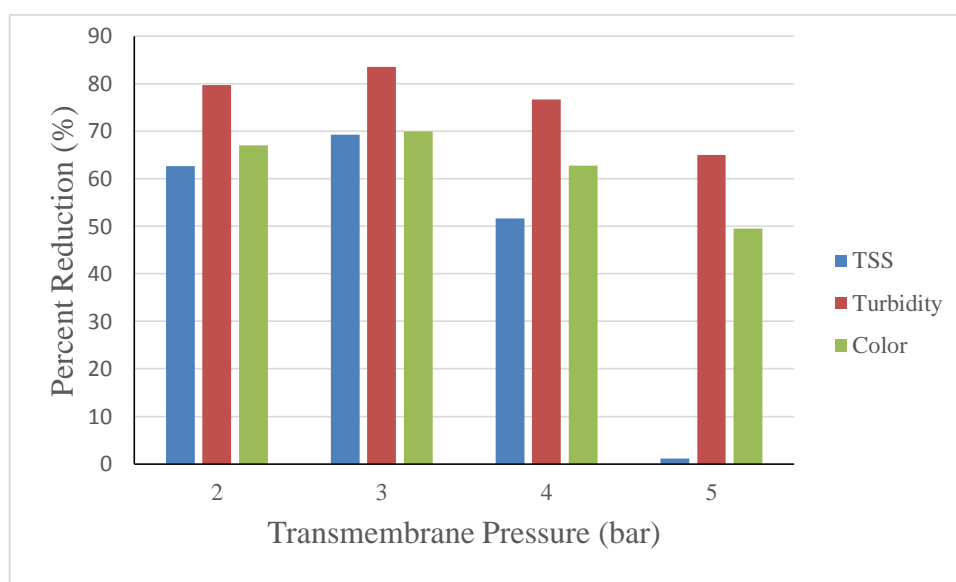


Figure 4.11: Percent Reduction of Total Suspended Solids, Turbidity and Colour for Membrane U1 under Different Transmembrane Pressures

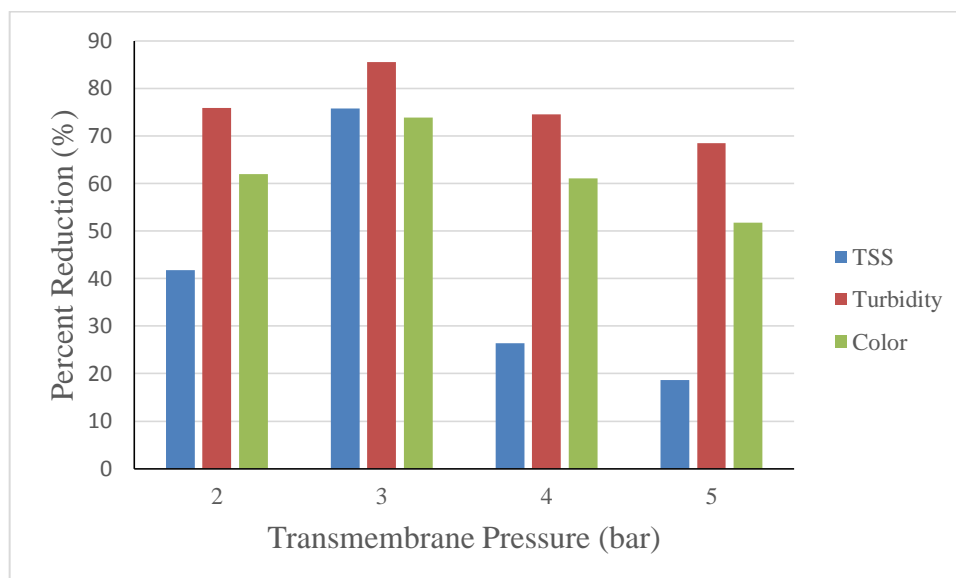


Figure 4.12: Percent Reduction of Total Suspended Solids, Turbidity and Colour for Membrane U2 under Different Transmembrane Pressures

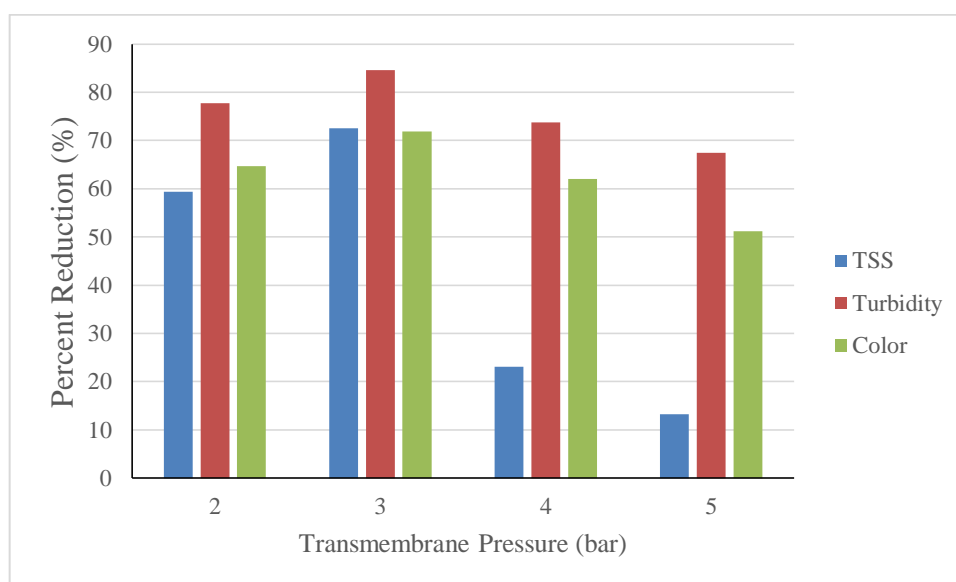


Figure 4.13: Percent Reduction of Total Suspended Solids, Turbidity and Colour for Membrane U3 under Different Transmembrane Pressures

4.4 Overall Reduction Percentage for Hybrid Process

The overall reduction percentage for the hybrid coagulation-ultrafiltration process for different membranes under 3 bar of TMP was depicted in Figure 4.14. The raw effluent was coagulated at the operating condition of pH 4, 600 mg/L of PAC and 200 rpm of rapid mixing speed. It was found that membrane U4 had the highest reduction of total suspended solids, turbidity and colour among other membranes at TMP of 3 bar. The percent reduction of total suspended solids, turbidity and colour were 99.95%, 99.21% and 98.60%, respectively. The increasing amount of TiO₂ nanoparticles in the membranes were said to have no contribution towards the reduction of TSS, turbidity and colour although it improved the permeate flux of membranes.

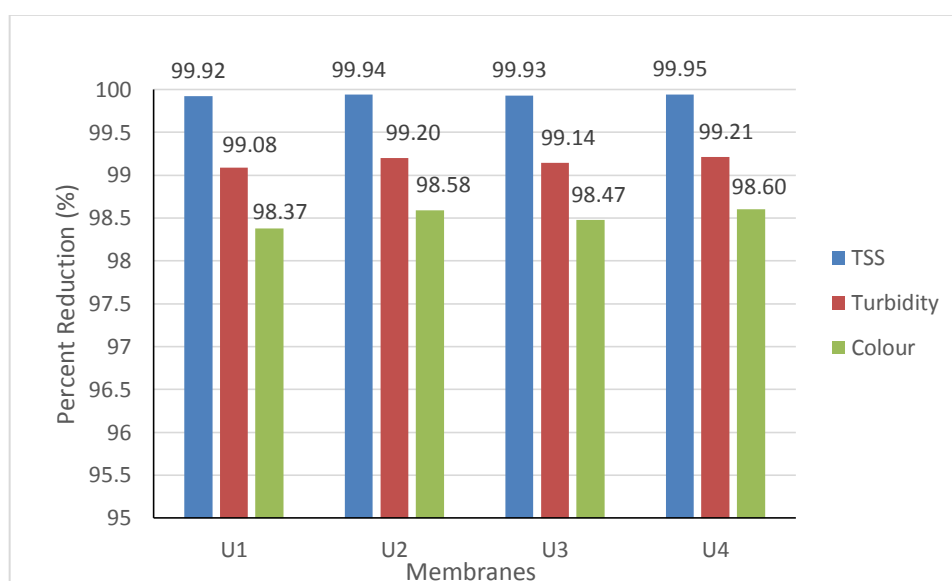


Figure 4.14: Overall Percent Reduction of Hybrid Coagulation-Ultrafiltration Process for Different Membranes under Transmembrane Pressure of 3 bar

4.5 Correlation of Total Suspended Solids, Turbidity and Colour

The relationships of total suspended solids, turbidity and colour were studied in Figures 4.15, 4.16 and 4.17. In Figures 4.15 and 4.16, the correlation of TSS with turbidity and colour were determined using the coefficient of determination (R^2). It was found that the R^2 value for TSS and turbidity was 0.8846, whereas for TSS and colour was 0.838, suggesting that a strong relationship between total suspended solids with both turbidity and colour. As mentioned earlier, the turbidity and colour in the POME were due to the existence of solids and organic matter in the solution. Therefore, removing solids in POME will give a reduction turbidity and colour in POME. However, the turbidity and colour in the POME may be contributed by other factors as the R^2 value did not approach to 1. Thus, the correlation of turbidity with colour was further identified to learn the contributing factor for both parameters.

The correlation of turbidity with colour is depicted in Figure 4.17. It was found that the R^2 value for both parameters was 0.9858, indicating that the turbidity and colour possessed an extremely strong relationship. The contributing factor for both parameters were assumed to be the same other than total suspended solids in POME. Thus, the contributing factor should be identified and removed in order to achieve a greater reduction of colour and turbidity in the POME.

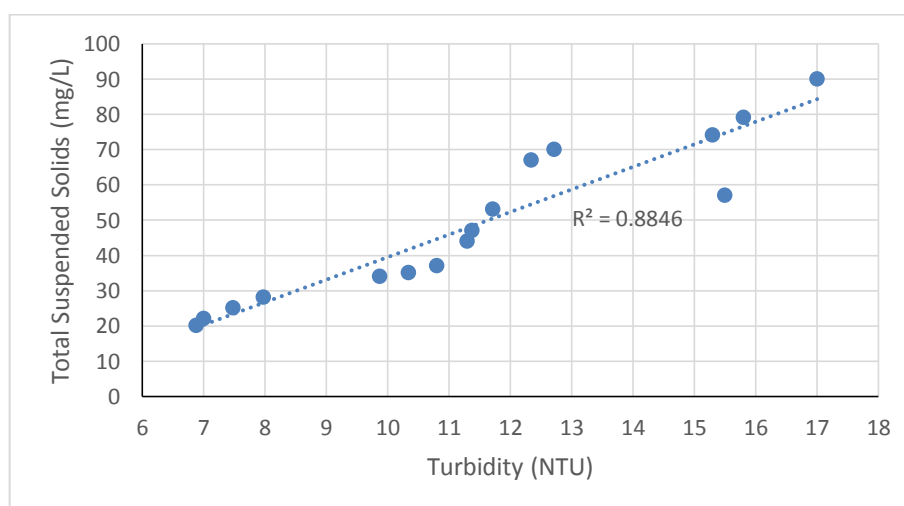


Figure 4.15: Correlation between Total Suspended Solids and Turbidity

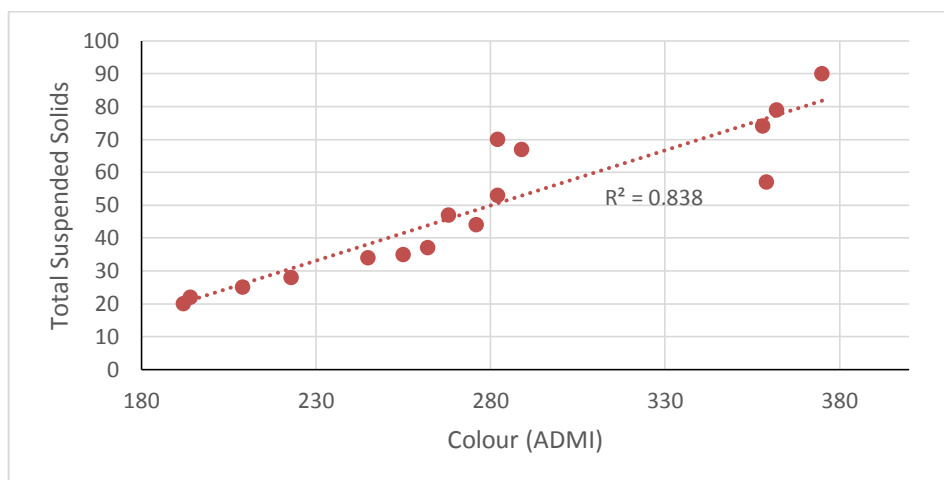


Figure 4.16: Correlation between Total Suspended Solids and Colour

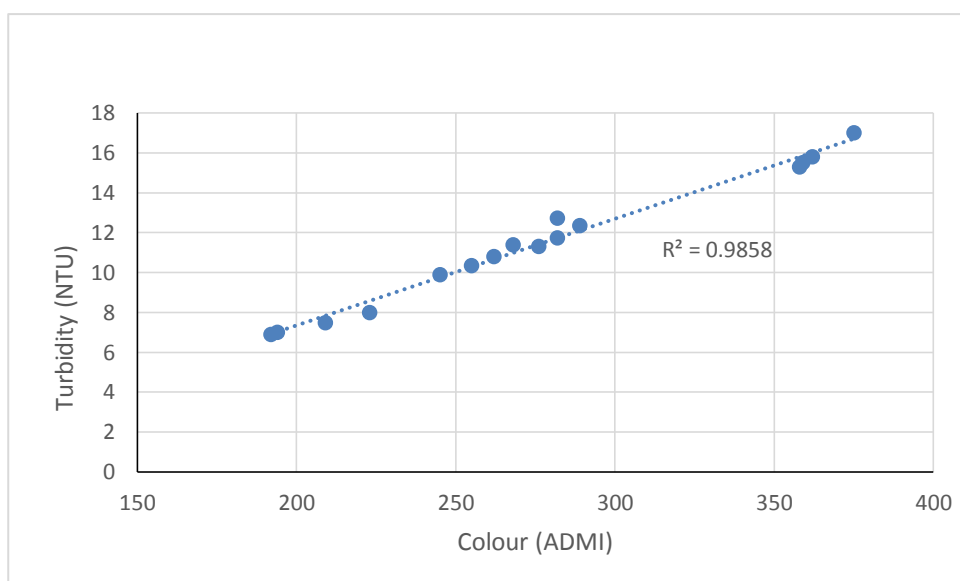


Figure 4.17: Correlation between Turbidity and Colour

CHAPTER 5

CONCLUSIONS AND RECOMMENDATIONS

5.1 Conclusions

In conclusion, the total suspended solids, turbidity and colour content were successfully reduced from anaerobically treated palm oil mill effluent (POME) using hybrid coagulation-ultrafiltration process. The operating conditions for coagulation using polyaluminium chloride were optimized at pH 4, 600 mg/L of coagulant and 200 rpm of rapid mixing speed. The percent reduction of total suspended solids, turbidity and colour from anaerobically treated POME via coagulation process were 99.74%, 94.44% and 94.60%, respectively.

Ultrafiltration (UF) membranes were fully characterized using SEM, EDX, porosity, pore size distribution and pure water permeability tests. The addition of titanium dioxide (TiO₂) nanoparticles greatly affected the characteristics of UF membranes. SEM micrograph images depicted that adding TiO₂ into membranes increased the size of finger-like macrovoid structure. The porosity and pore size of the UF membranes also increased with the addition of TiO₂, and hence promoting the pure water permeability and hydrophilicity of membranes.

The concentration of TiO₂ in the UF membranes only promoted the permeate flux of membranes while there were no effects on the reduction of total suspended solids, turbidity and colour due to the low concentration of TiO₂ added. The optimum transmembrane pressure (TMP) for membranes were found to be 3 bar at which the greatest percent reduction of total suspended solids, turbidity and colour was achieved. Further increasing TMP resulted in lower reduction percent reduction. The percent reduction of total suspended solids, turbidity and colour using membrane U4 at 4 bar TMP were 78.02%, 85.81% and 74.12%, respectively. The overall percent reduction for total suspended solids, turbidity and colour using hybrid coagulation-ultrafiltration process were 99.95%, 99.21% and 98.60%, respectively.

The turbidity and colour existed in POME was found to be correlated to total suspended solids due to high R² value. However, turbidity and colour in POME might be contributed by other factors as reduction of turbidity and colour do not achieve high reduction efficiencies when total suspended solids were removed from POME.

5.2 Recommendations for Future Work

There are several recommended researches. Firstly, natural coagulants can be utilized to coagulate POME as it is environmental friendly material and reduces environmental toxicity and hazards, but their preparation method and coagulation potential to achieve a greater reduction of total suspended solids, turbidity and colour need to be further investigated. Besides, higher amount of titanium dioxide nanoparticles can be added into membranes to investigate its effect on reduction of totals suspended solids, turbidity and colour from the POME. Lastly, contributing factor for turbidity and colour can be identified with further study in order to achieve a greater reduction of total suspended solids, turbidity and colour from the POME.

REFERENCES

- Advantages and Disadvantages of Reverse Osmosis - BIOTECH. [online] Available at: <https://www.biotechwater.com/advantages-disadvantages-reverse-osmosis/> [Accessed 19 Mar. 2018].
- A.L. Ahmad and C.Y. Chan, 2009. Sustainability of Palm Oil Industries: An Innovative Treatment via Membrane Technology. *Journal of Applied Sciences*, 9: 3074-3079.
- Ahmad, A., Chong, M., Bhatia, S. and Ismail, S. (2006). Drinking water reclamation from palm oil mill effluent (POME) using membrane technology. *Desalination*, 191(1-3), pp.35-44.
- Ahmad, A., Ismail, S. and Bhatia, S. (2003). Water recycling from palm oil mill effluent (POME) using membrane technology. *Desalination*, 157(1-3), pp.87-95.
- Ahmad, A., Sumathi, S. and Hameed, B. (2006). Coagulation of residue oil and suspended solid in palm oil mill effluent by chitosan, alum and PAC. *Chemical Engineering Journal*, 118(1-2), pp.99-105.
- Alkudhiri, A., Darwish, N. and Hilal, N. (2012). Membrane distillation: A comprehensive review. *Desalination*, 287, pp.2-18.
- Ahmed, S., Ayoub, G., Al-Hindi, M. and Azizi, F. (n.d.). The Effect of Fast Mixing Conditions on the Coagulation-Flocculation of Highly Turbid Suspensions Using Magnesium Hydroxide Coagulant.
- Ang, W., Mohammad, A., Hilal, N. and Leo, C. (2015). A review on the applicability of integrated/hybrid membrane processes in water treatment and desalination plants. *Desalination*, 363, pp.2-18.
- Arribas, P., Khayet, M., Garcia-Payo, M. and Gil, L. (2015). Novel and emerging membranes for water treatment by electric potential and concentration gradient membrane processes. *Advances in Membrane Technologies for Water Treatment*, [online] pp.288-295. Available at: <https://doi.org/10.1016/B978-1-78242-121-4.00009-5> [Accessed 18 Mar. 2018].
- Azmi, N. and Yunus, K. (2014). Wastewater Treatment of Palm Oil Mill Effluent (POME) by Ultrafiltration Membrane Separation Technique Coupled with Adsorption Treatment as Pre-treatment. *Agriculture and Agricultural Science Procedia*, [online] 2, pp.257-264. Available at: https://ac.els-cdn.com/S2210784314000382/1-s2.0-S2210784314000382-main.pdf?_tid=89a81db6-c4ec-4a07-aaf2-e4982fb0aab2&acdnat=1521270048_9272a81cc87a5b42884ea3c135ef3665 [Accessed 17 Mar. 2018].

Bakar, A. and Halim, A. (2013). Treatment of automotive wastewater by coagulation-flocculation using poly-aluminum chloride (PAC), ferric chloride (FeCl₃) and aluminum sulfate (alum).

Cao, X., Ma, J., Shi, X. and Ren, Z. (2006). Effect of TiO₂ nanoparticle size on the performance of PVDF membrane. *Applied Surface Science*, 253(4), pp.2003-2010

Cheryan, M. (2010). *Ultrafiltration and microfiltration*. Boca Raton [et al.]: CRC Press.

Chon, K., Cho, J., Kim, S. and Jang, A. (2014). The role of a combined coagulation and disk filtration process as a pre-treatment to microfiltration and reverse osmosis membranes in a municipal wastewater pilot plant. *Chemosphere*, 117, pp.20-26.

Department of Environment. (2015). https://www.doe.gov.my/portalv1/wp-content/uploads/2015/01/Peraturan_Kualiti_Alam_Sekeliling_Premis_Yang_Ditetapkan_Minyak_Sawit_Mentah_Pindaan_1982_-_P.U.A_183-82.pdf. [online] Available at: https://www.doe.gov.my/portalv1/wp-content/uploads/2015/01/Peraturan_Kualiti_Alam_Sekeliling_Premis_Yang_Ditetapkan_Minyak_Sawit_Mentah_Pindaan_1982_-_P.U.A_183-82.pdf [Accessed 19 Aug. 2018].

Ebeling, J., Sibrell, P., Ogden, S. and Summerfelt, S. (2003). Evaluation of chemical coagulation–flocculation aids for the removal of suspended solids and phosphorus from intensive recirculating aquaculture effluent discharge. *Aquacultural Engineering*, 29(1-2), pp.23-42.

Engelhardt, T. (2010). *Coagulation, Flocculation and Clarification of Drinking Water*. [online] Available at: https://www.researchgate.net/publication/265493759_Coagulation_Flocculation_and_Clarification_of_Drinking_Water [Accessed 21 Aug. 2018].

Farajnezhad, H. and Gharbani, P. (2012). Coagulation Treatment of Wastewater In Petroleum Industry Using Poly Aluminum Chloride And Ferric Chloride. [online] Available at: http://www.arpapress.com/Volumes/Vol13Issue1/IJRRAS_13_1_25.pdf [Accessed 25 Aug. 2018].

Field, R., Wu, D., Howell, J. and Gupta, B. (1995). Critical flux concept for microfiltration fouling. *Journal of Membrane Science*, 100(3), pp.259-272.

Hu, X., Bekassy-Molnar, E. and Koris, A. (2004). Study of modelling transmembrane pressure and gel resistance in ultrafiltration of oily emulsion. *Desalination*, 163(1-3), pp.355-360.

Hua, F., Tsang, Y., Wang, Y., Chan, S., Chua, H. and Sin, S. (2007). Performance study of ceramic microfiltration membrane for oily wastewater treatment. *Chemical Engineering Journal*, 128(2-3), pp.169-175.

Howe, K. and Clark, M. (2002). Coagulation pretreatment for membrane filtration. Denver, CO: AWWA Research Foundation and American Water Works Association.

Jafarinejad, S. (2017). Petroleum waste treatment and pollution control. Oxford: Butterworth-Heinemann is an imprint of Elsevier, p.215.

Jagaba, A.H, Latiff, A.A.A, Umaru, I, Abubakar, S. and Lwal, I.M., 2016. Treatment of POME using different Natural and Chemical Coagulants: A Review. IOSR Journal of Mechanical and Civil Engineering (E-journal). Vol. 13 (6), pp. 67-75. Available at: <http://www.iosrjournals.org/iosr-jmce/papers/vol13-issue6/Version-7/11306076775.pdf> [Accessed 18th August 2018]

Juholin, P. (2016). Hybrid Membrane Processes in Industrial Water Treatment. Separation and Recovery of Inorganic Compounds, [online] pp.29-33. Av

KIM, J., KANG, M. and KIM, C. (2005). Fabrication of membranes for the liquid separation Part 1. Ultrafiltration membranes prepared from novel miscible blends of polysulfone and poly(1-vinylpyrrolidone-co-acrylonitrile) copolymers. Journal of Membrane Science, 265(1-2), pp.167-175.

Juholin, P. (2016). Hybrid Membrane Processes in Industrial Water Treatment. Separation and Recovery of Inorganic Compounds, [online] pp.29-33. Available at: <http://jultika.oulu.fi/files/isbn9789526214412.pdf> [Accessed 18 Mar. 2018].

Kriipsalu, M., Marques, M., Nammari, D. and Hogland, W. (2007). Bio-treatment of oily sludge: The contribution of amendment material to the content of target contaminants, and the biodegradation dynamics. Journal of Hazardous Materials, 148(3), pp.616-622.

Li, J., Xu, Z., Yang, H., Yu, L. and Liu, M. (2009). Effect of TiO₂ nanoparticles on the surface morphology and performance of microporous PES membrane. Applied Surface Science, 255(9), pp.4725-4732.

Masoudnia, K., Raisi, A., Aroujalian, A. and Fathizadeh, M. (2013). Treatment of Oily Wastewaters Using the Microfiltration Process: Effect of Operating Parameters and Membrane Fouling Study. Separation Science and Technology, 48(10), pp.1544-1555.

Masoudnia, K., Raisi, A., Aroujalian, A. and Fathizadeh, M. (2014). A hybrid microfiltration/ultrafiltration membrane process for treatment of oily wastewater. Desalination and Water Treatment, 55(4), pp.901-912.

Mohammadi, T. and Esmaelifar, A. (2005). Wastewater treatment of a vegetable oil factory by a hybrid ultrafiltration-activated carbon process. Journal of Membrane Science, 254(1-2), pp.129-137.

Moosai, R. and Dawe, R. (2003). Gas attachment of oil droplets for gas flotation for oily wastewater cleanup. *Separation and Purification Technology*, 33(3), pp.303-314.

MPOB. (2014). Oil Palm & The Environment (updated March 2014). [online] Available at: <http://www.mpob.gov.my/en/palm-info/environment/520-achievements> [Accessed 19 Aug. 2018].

MPOC. (2012). Malaysian Palm Oil Industry. [online] Available at: http://www.m poc.org.my/Malaysian_Palm_Oil_Industry.aspx [Accessed 10 Apr. 2018].

Noble, R. and Stern, S. (2003). *Membrane separations technology*. Amsterdam: Elsevier, pp.1- 40.

Norulaini, N., Zuhair, A., Hakimi, M. and Kadir, M. (2001). Chemical Coagulation Of Settleable Solid-Free Palm Oil Mill Effluent (Pome) For Organic Load Reduction. *Journal of Industrial Technology*, [online] 10(1), pp.55-72. Available at: https://www.researchgate.net/publication/277123114_Chemical_Coagulation_Of_Settleable_Solid-Free_Palm_Oil_Mill_Effluent_Pome_For_Organic_Load_Reduction [Accessed 25 Aug. 2018].

Ong, C., Lau, W., Goh, P., Ng, B., Matsuura, T. and Ismail, A. (2014). Effect of PVP Molecular Weights on the Properties of PVDF-TiO₂ Composite Membrane for Oily Wastewater Treatment Process. *Separation Science and Technology*, 49(15), pp.2303-2314.

Orecki, A., Tomaszewska, M. and Karakulski, K. (2005). Removal of Oil from Model Oily Wastewater Using the UF/NF Hybrid Process. *Polish Journal of Environmental Studies*, [online] 15, pp.173-177. Available at: <http://www.pjoes.com/pdf/15.1/Pol.J.Enviro n.Stud.Vol.15.No.1.173-177.pdf> [Accessed 17 Mar. 2018].

OsmotechMembrane. (2018). Membrane Technology|Advantages of Membrane Technology|Membrane Producer – Osmotech Membrane Pvt. Ltd. Rajkot India. [online] Available at: <http://www.osmotechmembranes.com/membranes-layers> [Accessed 18 Mar. 2018].

Qu, P., Tang, H., Gao, Y., Zhang, L. and Wang, S. (2010). Polyethersulfone Composite Membrane Blended With Cellulose Fibrils. [online] Available at: http://ojs.cnr.ncsu.edu/index.php/BioRes/article/view/BioRes_05_4_2323_Qu_TGZ_W_Polyethersulfone_Membrane_Fibrils/739 [Accessed 21 Aug. 2018].

Regula, C., Carretier, E., Wyart, Y., Gésan-Guiziou, G., Vincent, A., Boudot, D. and Moulin, P. (2014). Chemical cleaning/disinfection and ageing of organic UF membranes: A review. *Water Research*, 56, pp.325-365.

Sadrzadeh, M., Gorouhi, E. and Mohammadi, T. (2008). Oily Wastewater Treatment Using Polytetrafluoroethylene (Ptfе) Hydrophobic Membranes.

Said, M., Ahmad, A., Mohammad, A., Nor, M. and Sheikh Abdullah, S. (2015). Blocking mechanism of PES membrane during ultrafiltration of POME. *Journal of Industrial and Engineering Chemistry*, 21, pp.182-188.

Salahi, A., Badrnezhad, R., Abbasi, M., Mohammadi, T. and Rekabdar, F. (2011). Oily wastewater treatment using a hybrid UF/RO system. *Desalination and Water Treatment*, 28(1-3), pp.75-82.

Salahi, A., Mohammadi, T., Mosayebi Behbahani, R. and Hemmati, M. (2015). Asymmetric polyethersulfone ultrafiltration membranes for oily wastewater treatment: Synthesis, characterization, ANFIS modeling, and performance. *Journal of Environmental Chemical Engineering*, 3(1), pp.170-178.

Singh, R. (2006). *Hybrid membrane systems for water purification*. Amsterdam: Elsevier.

Shi, X., Tal, G., Hankins, N. and Gitis, V. (2014). Fouling and cleaning of ultrafiltration membranes: A review. *Journal of Water Process Engineering*, 1, pp.121-138.

Synderfiltration. (2018). *Membrane Materials: Organic v. Inorganic*. [online] Available at: <http://synderfiltration.com/learning-center/articles/introduction-to-membranes/membrane-materials-organic-inorganic/> [Accessed 27 Mar. 2018].

Teh, C., Budiman, P., Shak, K. and Wu, T. (2016). Recent Advancement of Coagulation–Flocculation and Its Application in Wastewater Treatment. *Industrial & Engineering Chemistry Research*, 55(16), pp.4363-4389.

Terefe, S., Glagovskaia, O., Janakievski, F., Silva, K., Horne, M. and Stockmann, R. (2018). Forward Osmosis: A Novel Membrane Separation Technology of Relevance to Food and Related Industries. *Innovative Food Processing Technologies*.

Thuyavan, Y., Anantharaman, N., Arthanareeswaran, G. and Ismail, A. (2016). Impact of solvents and process conditions on the formation of polyethersulfone membranes and its fouling behavior in lake water filtration. *Journal of Chemical Technology & Biotechnology*, 91(10), pp.2568-2581.

Ujang, F., Osman, N., Idris, J., Halmi, M., Hassan, M. and Roslan, A. (2018). Start-up treatment of palm oil mill effluent (POME) final discharge using Napier Grass in wetland system. *IOP Conference Series: Materials Science and Engineering*, 368, p.012008.

YAN, L., LI, Y., XIANG, C. and XIANDA, S. (2006). Effect of nano-sized Al₂O₃-particle addition on PVDF ultrafiltration membrane performance. *Journal of Membrane Science*, 276(1-2), pp.162-167..

Yu, L., Han, M. and He, F. (2017). A review of treating oily wastewater. *Arabian Journal of Chemistry*, 10, pp.S1913-S1922.

Zainal, N. (2018). A Review On The Development Of Palm Oil Mill Effluent (Pome) Final Discharge Polishing Treatments. *Journal of Oil Palm Research*, 29(4), pp.528-540.

Zhang, W., Luo, J., Ding, L. and Jaffrin, M. (2015). A Review on Flux Decline Control Strategies in Pressure-Driven Membrane Processes. ACS publication.

Zhao, Y., Wu, K., Wang, Z., Zhao, L. and Li, S. (2000). Fouling and Cleaning of membrane- A literature review. *Journal of Environmental Sciences*, 12(2), pp.241-251.

APPENDICES

APPENDIX A: Coagulation Data

Table A.1: Initial TSS, Turbidity and Colour for Raw POME

Parameters	Values
Total Suspended Solids, mg/L	36000
Turbidity, NTU	873
Colour, ADMI	13740

Table A.2: TSS, Turbidity and Colour Data for Coagulated POME under Different pH

Conditions			Parameters		
Dosage of Coagulant (mg/L)	Rapid Mixing Speed (rpm)	pH	TSS (mg/L)	Turbidity (NTU)	Colour (ADMI)
600	150	2	310	188	1253
		3	334	189	1235
		4	119	6802	845
		5	483	245	1654
		6	510	245	1643
		7	530	279	1677
		8	474	244	1621
		9	443	240	1628

Table A.3: TSS, Turbidity and Colour Data for Coagulated POME under Different Dosage of Coagulant

Conditions			Parameters		
pH	Rapid Mixing Speed (rpm)	Dosage of Coagulant (mg/L)	TSS (mg/L)	Turbidity (NTU)	Colour (ADMI)
4.0	150	200	528	270.0	1668
		400	170	96.1	1013
		600	78	44.4	687
		800	137	69.7	890
		1000	167	94.2	970

Table A.4: TSS, Turbidity and Colour Data for Coagulated POME under Different Rapid Mixing Speed

Conditions			Parameters		
pH	Dosage of Coagulant (mg/L)	Rapid Mixing Speed (rpm)	TSS (mg/L)	Turbidity (NTU)	Colour (ADMI)
4.0	600	100	245	141	1204
		150	68.2	119	845
		200	91	48.5	742
		250	164	84.5	962

APPENDIX B: EDX Analysis

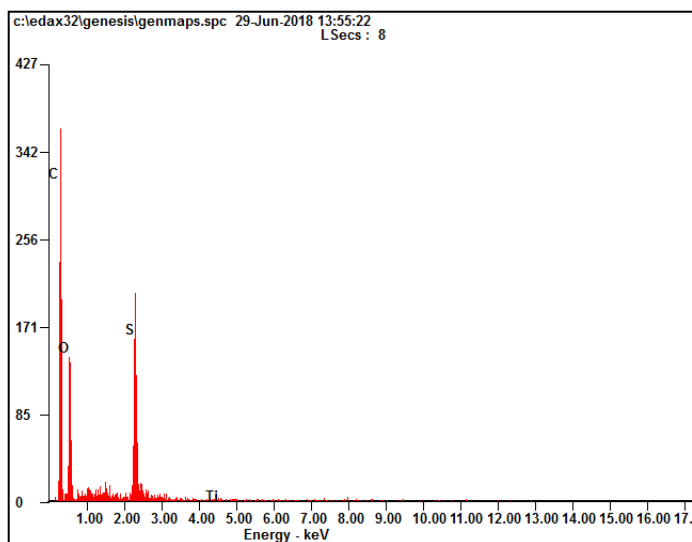


Figure B.1: Chemical Composition of U1

Table B.1: Chemical Composition of U1

<i>Element</i>	<i>Wt%</i>	<i>At%</i>
<i>CK</i>	61.16	70.40
<i>OK</i>	29.70	25.66
<i>SK</i>	09.14	03.94
<i>TiK</i>	00.00	00.00
<i>Matrix</i>	Correction	ZAF

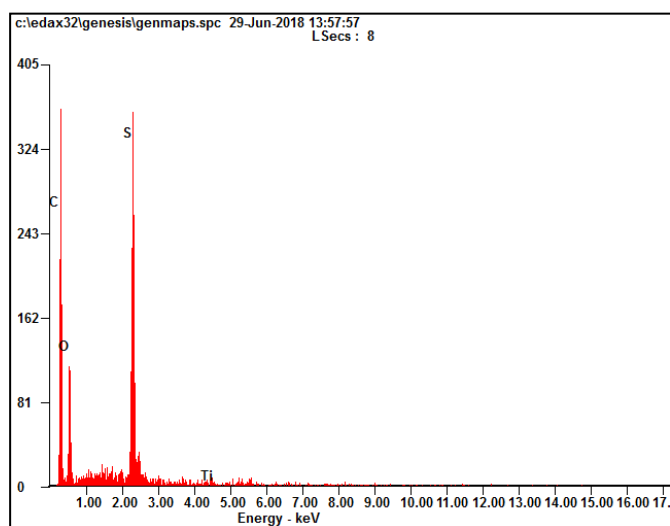


Figure B.2: Chemical Composition of U2

Table B.2: Chemical Composition of U2

<i>Element</i>	<i>Wt%</i>	<i>At%</i>
<i>CK</i>	62.08	73.28
<i>OK</i>	22.56	20.00
<i>SK</i>	14.89	06.59
<i>TiK</i>	00.46	00.14
<i>Matrix</i>	Correction	ZAF

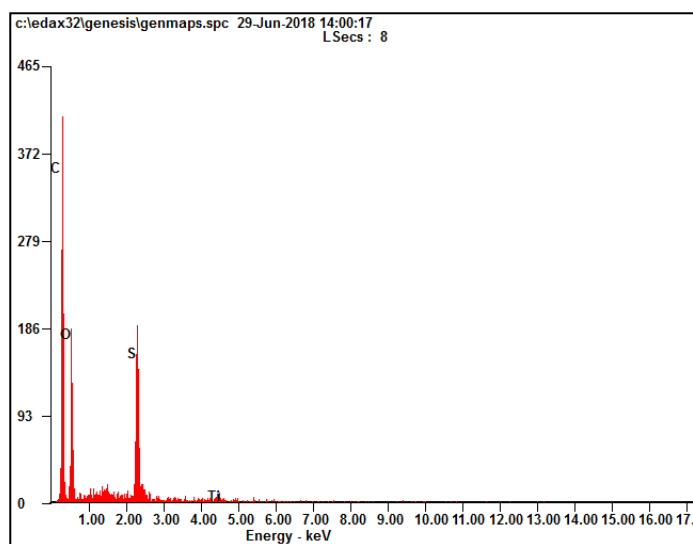


Figure B.3: Chemical Composition of U3

Table B.3: Chemical Composition of U3

<i>Element</i>	<i>Wt%</i>	<i>At%</i>
<i>CK</i>	60.19	69.54
<i>OK</i>	30.65	26.59
<i>SK</i>	08.51	03.68
<i>TiK</i>	00.65	00.19
<i>Matrix</i>	Correction	ZAF

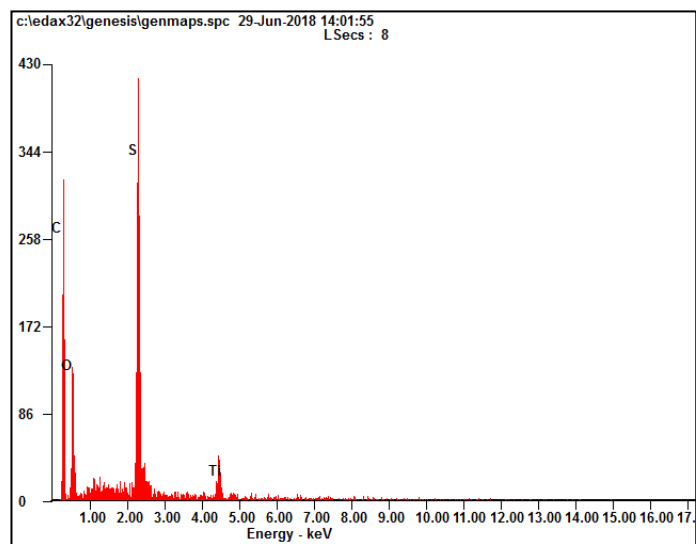


Figure B.4: Chemical Composition of U4

Table B.4: Chemical Composition of U4

<i>Element</i>	<i>Wt%</i>	<i>At%</i>
<i>CK</i>	57.05	70.17
<i>OK</i>	22.96	21.20
<i>SK</i>	16.19	07.46
<i>TiK</i>	03.80	01.17
<i>Matrix</i>	Correction	ZAF

APPENDIX C: Wet and Dry Weight of Membranes

Table C.1: Wet weight of Membranes

Membrane	Wet Weight of Membranes (g)			Average Wet Weight(g)
	Run			
	1	2	3	
U1	0.2206	0.2716	0.2112	0.2344
U2	0.2440	0.3500	0.3820	0.3253
U3	0.1968	0.4130	0.3290	0.3129
U4	0.2847	0.3526	0.2459	0.2944

Table C.2: Wet weight of Membranes

Membrane	Dry Weight of Membranes (g)			Average Dry Weight(g)
	Run			
	1	2	3	
U1	0.047	0.0395	0.0482	0.0449
U2	0.0511	0.0590	0.0476	0.0525
U3	0.0428	0.0528	0.0373	0.0443
U4	0.035	0.0424	0.044	0.0404

APPENDIX D: Membrane Filtration Data

Table D.1: TSS, Turbidity and Colour after Filtration by Membrane U1 under Different Pressure

Pressure (bar)	Total Suspended Solids (mg/L)	Turbidity (NTU)	Colour (ADMI)
2	34	9.87	245
3	28	7.98	223
4	44	11.30	276
5	90	17.00	375

Table D.2: TSS, Turbidity and Colour after Filtration by Membrane U2 under Different Pressure

Pressure (bar)	Total Suspended Solids (mg/L)	Turbidity (NTU)	Colour (ADMI)
2	53	11.72	282
3	22	7.00	194
4	67	12.34	289
5	74	15.30	358

Table D.3: TSS, Turbidity and Colour after Filtration by Membrane U3 under Different Pressure

Pressure (bar)	Total Suspended Solids (mg/L)	Turbidity (NTU)	Colour (ADMI)
2	37	10.80	262
3	25	7.48	209
4	70	12.72	282
5	79	15.80	362

Table D.4: TSS, Turbidity and Colour after Filtration by Membrane U4 under Different Pressure

Pressure (bar)	Total Suspended Solids (mg/L)	Turbidity (NTU)	Colour (ADMI)
2	35	10.34	255
3	20	6.88	192
4	47	11.38	268
5	57	15.50	359